A Generalized Analysis of Multiple-Clad Optical Fibers with Arbitrary Step-Index Profiles and Applications

by

Taha Mohamed Barake

Thesis submitted to the Faculty of the
Virginia Polytechnic Institute and State University
in partial fulfillment of the requirements for the degree of
Master of Science
in
Electrical Engineering

APPROVED:

A. Safaai-Jazi

Dr. Ahmad Safaai-Jazi, Chairman

Lee Johnson

Dr. Lee Johnson

Dr. Ioannis M. Besieres

April 1997
Blacksburg, Virginia
Keywords: Multiple-Clad Fibers, Dispersion-Altered Fibers

A Generalized Analysis of Multiple-Clad Optical Fibers with Arbitrary Step-Index Profiles and Applications

by

Taha Barake

Committee Chairman: Dr. Ahmad Safaai-Jazi

Electrical Engineering

(ABSTRACT)

A generalized analysis of multiple-clad cylindrical dielectric structures with step-index profiles is presented. This analysis yields unified expressions for fields, dispersion equation and cutoff conditions for weakly guiding optical fibers with step-index but otherwise arbitrary profiles. The formulation focuses on triple-clad fibers, but can accommodate single and double-clad fibers as special limiting cases.

Using the generalized solutions, transmission properties of several types of specialty fibers for broadband applications, including dispersion-shifted, dispersion-flattened, and dispersion compensating fibers, are studied. Improved designs for dispersion-shifted and dispersion compensating fibers are achieved.

Fiber parameters and material compositions for the improved designs are provided. The proposed design for the dispersion-shifted fiber yields zero second-order as well as third-order dispersion at the $\lambda = 1.55 \mu m$ wavelength. The dispersion compensating fiber proposed here provides a large negative dispersion of about $-400\, ps/nm.km$ at $\lambda = 1.55 \mu m$ for the fundamental mode. Numerical results for dispersion characteristics, cutoff wavelengths, and radial field distributions are provided.

Acknowledgments

First and foremost, I thank God for his guidance and for blessing me with the special people who helped and supported me so much and for so long. I wish to extend my most sincere thanks and great gratitude to my advisor Dr. Ahmad Safaai-Jazi for his tireless efforts and unending caring and generosity. I shall forever cherish his friendship. I also would like to thank the members of my committee Dr. Ioannis Besieres and Dr. Lee Johnson for what they have taught me and for always being so eager to help.

I would also like to thank my wonderful parents, sisters, and my dear brother for everything they had to go through so I can be where I am today, and to them I dedicate this thesis.

Table of Contents

List of Figures

List of Tables

Chapter 1. Introduction

Optical fibers with modified dispersion characteristics, such as dispersion-shifted, dispersion-flattened, and dispersion compensating fibers, are of considerable interest in broadband fiber-optic communication systems. Dispersion-shifted fibers offer a very small dispersion at the wavelength of $\lambda = 1.55 \mu m$. This wavelength corresponds to the minimum attenuation wavelength of silica-based optical fibers. Thus, dispersion-shifted fibers cause much less signal distortion and attenuation than ordinary single-mode fibers [1-3]. Dispersion-flattened fibers provide small dispersion over an extended range of wavelengths. These fibers have application in wavelength-division multiplexed systems in which several optical channels are simultaneously transmitted on the same fibers. With a flattened dispersion characteristic, all channels suffer small signal distortions [4-5]. Both dispersion-shifted and dispersion-flattened fibers are single-mode with multiple cladding geometries. Their propagation properties have been studied extensively in the past [6-8].

Unlike dispersion-shifted and dispersion-flattened fibers which are desired to have very small dispersion at $\lambda = 1.55 \mu m$, dispersion compensating fibers are designed to provide very large negative dispersion at this wavelength. These fibers are used to upgrade the $1.3 \mu m$ fiber-optic links. Optical fibers designed for use at $1.3 \mu m$ wavelength may be operated at $1.55 \mu m$ in order to take advantage of lower the fiber attenuation at this wavelength. However, such fibers at $1.55 \mu m$ have fairly large positive dispersion which results in signal distortion. To compensate for the accumulated dispersion over the length of

the link, the fiber is concatenated with a shorter length of a dispersion compensating fiber with large negative dispersion. Most dispersion compensating fibers reported in the literature have a single cladding layer and operate in LP_{01} or LP_{11} mode [9-11].

Although much work has been done on the analysis and design of fibers with modified dispersion characteristics, little has been reported on the optimization of their designs. For example, dispersion-shifted fibers provide a nominal zero dispersion at $\lambda = 1.55 \mu m$. However, it is understood that only the second-order dispersion vanishes at $1.55 \mu m$ in these fibers, and third and higher-order dispersions exist and contribute to signal distortion. An optimum design will not only provide zero second-order but also zero third-order dispersion. (Fourth and higher-order dispersions are very small and neglected). For the case of dispersion compensating fibers operating in the LP_{11} mode, there are difficulties with mode conversion, because such fibers are dual mode. A more practical design is a single-mode dispersion compensating fiber. Moreover, the amount of negative dispersion should be as large as possible in order to reduce the required length of such fibers.

In this thesis, improved designs for dispersion-shifted and dispersion compensating fibers are presented. A triple-clad cylindrical dielectric structure is used as a common geometry for all fiber designs. The refractive index profile is determined based on design requirements. A new dispersion-shifted fiber is proposed which provides zero second-order as well as third-order dispersion. The advantage of this fiber over the conventional dispersion-shifted fiber is in its zero third-order dispersion. Also, a dispersion compensating fiber is designed which provides a dispersion of about $-400 \, ps / nm.km$ at $\lambda = 1.55 \mu m$. The important aspect of this design is that this large negative dispersion is associated with the fundamental LP_{01} mode and hence problems of mode coupling encountered in dual-mode dispersion compensating fibers are avoided. In addition to dispersion-shifted and dispersion compensating designs mentioned above, the triple-clad

geometry is used to obtain a dispersion-flattened design with less than $1 ps/nm.km$ chromatic dispersion over the $1.38 \mu m - 1.59 \mu m$ wavelength range.

Another contribution of this work is a generalized field analysis of triple-clad cylindrical dielectric structures. This generalized solution can accommodate all possible triple-clad fibers with step-index profiles. Accordingly, the analysis and design of the proposed dispersion-shifted, dispersion-flattened, and dispersion compensating fibers are performed using a single unified formulation. The formulation can also treat various double-clad configurations and the single-clad fiber as special cases in which the thickness of one or more layers becomes arbitrarily small. This generalized formulation lends itself to straightforward computer algorithms and code development for the calculation of propagation properties of single, double, and triple-clad fibers.

The outline of the remaining chapters of this thesis is as follows. Chapter two addresses various dispersion mechanisms in optical fibers. Dispersion-altered fibers and their applications are discussed. The effect of attenuation on dispersion is also briefly examined. Chapter three is devoted to a generalized analysis of multiple-clad fibers. Scalar field solutions, characteristic equation, and cutoff conditions for guided modes are presented. Numerical results for variations of normalized propagation constant as well as chromatic dispersion versus wavelength and radial field distributions are provided in chapter four. Parameters and material compositions for four fibers are presented. These fibers represent examples of dispersion-shifted fiber with only zero second-order dispersion, optimized dispersion-shifted fiber with zero second-order and third-order dispersions, dispersion-flattened fiber, and dispersion compensating fiber. Chapter five summarizes the conclusions of this research and points out directions for further investigations.

Chapter 2. Dispersion in Optical Fibers

An information signal becomes distorted due to attenuation and dispersion as it travels in an optical fiber. Attenuation is the loss of signal power and is governed by different mechanisms, including absorption, scattering, and radiation. Since optical fibers were introduced for communication applications three decades ago, great progress has been accomplished in producing optical fibers that exhibit very low signal attenuation. On the other hand, dispersion is the spreading in the time domain of a signal pulse as it travels through the fiber. Spectral components of a pulse propagating down an optical fiber reach their destination at slightly different times. This translates into a wider pulse at the receiving end of the fiber. Both attenuation and dispersion affect repeater spacing in a long distance fiber-optic communication system. Dispersion affects the bandwidth of the system, hence maintaining low dispersion is of equal importance for ensuring increased system information capacity, versatility and cost effectiveness.

2.1 Dispersion in Single-Mode Fibers

Dispersion in single-mode fibers is an intramodal effect and is a result of group velocity dependence on wavelength. Because of that, the amount of signal distortion depends on the spectral width of the optical source used. Three mechanisms contribute to intramodal dispersion: material dispersion, waveguide dispersion, and polarization-mode dispersion.

2.1.1 Material Dispersion

Material dispersion is caused by variations of refractive index of the fiber material with respect to wavelength. Since the group velocity is a function of the refractive index, the spectral components of any given signal will travel at different speeds causing deformation of the pulse. Variations of refractive index with respect to wavelength are described by the Sellmeier equation which is expressed as follows [12]

$$n(\lambda) = \left[1 + \sum_{i=1}^{3} \frac{A_i \lambda^2}{(\lambda^2 - \lambda_i^2)}\right]^{1/2}, \qquad (2.1)$$

where λ is the wavelength of light, and A_i and λ_i are the Sellmeier coefficients, and are tabulated in [12] and [13] for a number of silica-based glass materials commonly used in fabrication of optical fibers.

2.1.2 Waveguide Dispersion

Waveguide dispersion occurs because different spectral components of a pulse travel with different velocities by the fundamental mode of the fiber. It is as a result of axial propagation constant β being a function of wavelength due to the existence of one or more boundaries in the structure of the fiber. Without such boundaries, the fiber reduces to a homogeneous medium, the fundamental mode becomes a uniform plane-wave, and the waveguide dispersion effect is eliminated.

2.1.3 Polarization-Mode Dispersion

Single-mode fibers, in reality, support two orthogonally-polarized fundamental modes. In perfectly circular fibers, these two modes have identical propagation constants and pulse spreading due to polarization-mode dispersion does not exist. In practical fibers, however, there is a small difference between the propagation constants of these two modes

due to the slight ellipticity of the core. In other words, common single-mode fibers actually support two modes and thus are not truly single-mode. The presence of two fundamental modes contributes to pulse spreading. This phenomenon is known as polarization-mode dispersion.

2.2 Dispersion in Multimode Fibers

In applications where two or more modes travel simultaneously though the fiber, intermodal as well as intramodal dispersions exist. Intermodal dispersion does not occur in single-mode fibers, but is a significant effect in multimode fibers. It occurs as a result of different modes having different group velocities at the same frequency. Graded-index fibers with nearly parabolic-index profile were developed mainly to reduce the effect of intermodal dispersion. Here, bound rays deviating from the axis of the fiber travel a longer distance but at larger velocities, reaching the receiving end of the fiber at about the same time with the other rays, thus in graded-index fibers pulse spreading is significantly reduced.

Although all forms of dispersion present in single-mode fibers exist in multimode fibers too, the material dispersion is the only significant intramodal effect which should be considered. Thus, pulse spreading in multimode fibers is largely due to material dispersion and intermodal delay distortion. Polarization-mode dispersion is a much weaker effect than material dispersions and intermodal delay, and is often neglected in the analysis and design of fiber-optic links.

Apart from the three dispersion effects described above, there is yet another kind of dispersion referred to as profile dispersion. This effect is attributed to core and cladding materials having slightly different material dispersions. In this thesis, the profile dispersion is accounted for as part of material dispersion and thus does not require a separate analysis.

2.3 Group Velocity, Group Delay, and Dispersion

Let us consider an information signal propagating in a single-mode fiber of length L. Each spectral component of the signal undergoes a time delay t_g. The time delay per unit length, denoted as τ_g, is obtained as

$$\tau_g = \frac{t_g}{L} = \frac{1}{v_g} = \frac{1}{c}\frac{d\beta}{dk_0} = \frac{-\lambda^2}{2\pi c}\frac{d\beta}{d\lambda} \tag{2.2}$$

where $v_g = (d\beta / d\omega)^{-1} = c(d\beta / dk_0)^{-1}$ is the group velocity, $k_0 = 2\pi / \lambda$ is the free-space wave number, and c is the velocity of light in free space. Spectral components travel at different speeds and experience different time delays. We are interested in the pulse spreading arising from group delay variations. Let the root-mean-square spectral width of the optical source be σ_λ, then the total delay difference is given by

$$\delta\tau = \frac{d\tau_g}{d\lambda}\sigma_\lambda L \tag{2.3}$$

The amount of pulse spread per unit length of fiber and per unit spectral width of light source is defined as dispersion. Thus, the expression of dispersion is written as

$$D = \frac{1}{L\sigma_\lambda}\delta\tau = \frac{d\tau_g}{d\lambda} = -\frac{\lambda}{2\pi c}\left(2\frac{d\beta}{d\lambda} + \lambda\frac{d^2\beta}{d\lambda^2}\right) \tag{2.4}$$

A more suitable formula for calculation of dispersion is that expressed in terms of the normalized propagation constant $\overline{\beta}$, defined as $\overline{\beta} = \beta / k_0 = 2\pi\beta / \lambda$. Substituting for β, in terms of $\overline{\beta}$, (2.4) is reduced to

$$D = -\frac{\lambda}{c}\frac{d^2\overline{\beta}}{d\lambda^2} \tag{2.5}$$

The cumulative effect of waveguide and material dispersion is usually referred to as chromatic dispersion. Chromatic dispersion in ordinary single-mode fibers is approximated by adding the material and waveguide dispersion effects determined separately. This

approximation, while satisfactory for ordinary single-mode fibers, may not be adequate for ultra-low dispersion fibers such as dispersion-shifted and dispersion-flattened fibers [6-7]. Therefore, for better accuracy, material and waveguide dispersion effects are calculated simultaneously. In doing so, the wavelength dependence of the refractive index of each material is accounted for when determining the propagation constant β. The propagation constant is calculated by numerically solving the characteristic equation which may be expressed as $f(\lambda, \beta, n_i, i = 1,2,\ldots,N) = 0$, for a fiber consisting of N layers. The function f also includes variables such as core and cladding radii, which are independent of wavelength, and the azimuthal mode number. The refractive indices n_i are determined using the Sellmeier equation given in (2.1). Using numerical techniques, $\overline{\beta}$, $d\overline{\beta}/d\lambda$, $d^2\overline{\beta}/d\lambda^2$ are determined and put in (2.5) to obtain the total dispersion. It is emphasized that using this method of calculation, waveguide, material, and profile dispersion effects are simultaneously accounted for.

2.4 Dispersion-Altered Fibers

The objective in the optimum design of an optical fiber is to achieve the lowest attenuation and dispersion at the wavelength of operation. In ordinary single-mode fibers, total dispersion vanishes at a wavelength of about $1.3\,\mu m$. However, the lowest attenuation for glass fibers occurs at $1.55\,\mu m$. Alteration of dispersion in a fiber is attained by manipulating the index profile and geometry of the fiber. Dispersion-altered fibers include dispersion-shifted, dispersion-flattened, and dispersion compensating fibers discussed below.

2.4.1 Dispersion-Shifted Fibers

Dispersion-shifted fibers are the type in which the wavelength of zero dispersion is shifted to the region of lowest attenuation, which for $SiO_2 - GeO_2$ based fibers lies in the

1.55 μm region [1] and [21-22]. Providing minimal dispersion over a very narrow range of wavelengths, dispersion-shifted fibers are best suited for single channel transmission. The system's efficiency is increased due to longer repeater spacing, one of the most important considerations in designing long-distance optical fiber communication systems. Multiclad fibers with step-index, as well as graded cores can be used to design dispersion-shifted single-mode fibers [2] and [14].

2.4.2 Dispersion-Flattened Fibers

The possibility of low dispersion over an extended range of wavelengths was presented by Kawakami and Nishida in 1974 [15], and studied extensively thereafter [6] and [23]. By manipulating the index profile of a fiber, total dispersion can be made to go to zero at two or three different wavelengths, and remain close to zero in between. Dispersion flattening occurs by partial cancellation of waveguide dispersion by material dispersion in the wavelength range of operation. In some applications such as wavelength division multiplexing, where a number of signals with different wavelengths are carried by one fiber, it is desired to design the fiber optic system such that all optical signals experience relatively the same low distortion. The information capacity of fiber-optic systems using dispersion-flattened fibers and wavelength division multiplexing (WDM) schemes can be increased many folds. Multiclad fibers, including double, triple, and quadruple-clad fibers can be used to design dispersion-flattened fibers. Fiber designs have been reported where dispersion is less than 1 ($ps/nm.km$) over the entire range 1.31 μm to 1.67 μm [16].

2.4.3 Dispersion Compensation

The performance of a long distance optical fiber communication system is limited by various factors, one of which is dispersion, as mentioned earlier. Pulse distortion reduces maximum spacing between optical transmitters and receivers if the same BER performance for the system is to be maintained.

When commercial single-mode optical fiber links were first introduced and installed, they were designed to offer zero dispersion at $1.3\mu m$, since that was the wavelength of commercially available light sources. Operated nowadays at $1.55\mu m$, these fibers exhibit substantial positive dispersion that may be canceled out by using dispersion compensating fibers which provide large negative dispersion at that wavelength [9-10].

A signal traveling through an old-generation single-mode fiber link suffers a total dispersion DL over a distance L, where D is the dispersion per unit length, described earlier in equation (2.5), measured at $1.55\mu m$. DL maybe be of considerable magnitude after a long distance is traveled. Dispersion compensation is realized by splicing an optical fiber of length l that exhibits large negative dispersion, D', at the wavelength of operation, such that $D'l$ cancels out DL; that is $DL + D'l = 0$. The length of the compensating fiber needed l is thus obtained from $l = |D / D'|L$. Dispersion compensating fibers make it possible to upgrade existing $1.3\mu m$ links without unnecessary and expensive replacements.

2.5 Effect of Attenuation on Dispersion

When calculating dispersion in an optical fiber, it is commonly assumed that the fiber is lossless. In other words, the refractive indices of various layers constituting the fiber are all assumed to be real. In reality, these indices are complex with small imaginary parts which account for the losses in the fiber. The effect of losses on dispersion is generally negligible. However, it seems that no investigation has been made to verify how small this effect may be and if it might have to be considered in ultra-low dispersion fibers. Here, the effect of attenuation on dispersion is assessed using a perturbation approach.

If the scalar field of a lossless weakly guiding fiber of refractive index profile n is ψ and that of a low-loss fiber with refractive index $\hat{n}$ is $\hat{\psi}$, it can be shown that [17]

$$\beta^2 - \hat{\beta}^2 = k_0^2 \frac{\int_S (n^2 - \hat{n}^2)\psi\hat{\psi}ds}{\int_S \psi\hat{\psi}ds} \tag{2.6}$$

where β and $\hat{\beta}$ are the propagation constants of the lossless and the low-loss fibers respectively, S is a z=constant plane (assuming that the z-axis coincides with the fiber axis), and $k_0 = 2\pi / \lambda$ is the free-space wave number. Here, the low-loss fiber is regarded as a perturbation of the lossless fiber. The refractive index n is real, while $\hat{n}$ is complex with a small imaginary part accounting for fiber losses. n and $\hat{n}$ differ only in the imaginary part of $\hat{n}$. That is $\hat{n} = n - j\delta n$, $\delta n << n$. It is clear that β and $\hat{\beta}$ also differ by a small amount, and we can write $\hat{\beta} = \beta + \delta\beta$; $|\delta\beta| << \beta$.

Substituting for $\hat{\beta}$ and $\hat{n}$ in terms of β and n, respectively, and also using $\psi \cong \hat{\psi}$, from (2.6) we obtain

$$\delta\beta = -\frac{k_0^2}{2\beta} \frac{\int_S (j2n\delta n + \delta n^2)\psi^2 ds}{\int_S \psi^2 ds} \tag{2.7}$$

The imaginary part of $\delta\beta$, denoted as $-\alpha$, is in fact the attenuation coefficient of the fiber,

$$\alpha = \frac{k_0^2}{\beta} \frac{\int_S n\delta n\psi^2 ds}{\int_S \psi^2 ds} \tag{2.8}$$

while the real part of $\delta\beta$ is

$$\delta\beta_r = -\frac{k_0^2}{\beta} \frac{\int_S \delta n^2 \psi^2 ds}{\int_S \psi^2 ds} \tag{2.9}$$

For weakly guiding fibers n, $\hat{n}$, and δn vary very slowly over the fiber cross section and thus may be assumed as nearly constant. This approximation essentially amounts to considering the fiber as a homogeneous medium. Here, we are content with this approximation, because our purpose is to assess the order of magnitude of the attenuation effect on dispersion. One can always use (2.8) and (2.9) for a more accurate evaluation of this effect. Using this approximation and noting that $k_0 n \cong \beta$, we obtain

$$\alpha \cong \frac{k_0^2 n \delta n}{\beta} \cong k_0 \delta n \tag{2.10}$$

$$\delta\beta_r \cong -\frac{k_0^2}{2\beta}\delta n^2 = -\frac{\alpha^2\beta}{2k_0^2 n^2} = \frac{-\alpha^2\overline{\beta}}{2k_0 n^2} \tag{2.11}$$

where $\overline{\beta} = \beta / k_0$.

A change in the amount of $\delta\beta_r$ in β brings about a change in the dispersion, δD, which can be calculated from (2.5) as follows

$$\delta D = -\frac{\lambda}{c}\frac{d^2(\delta\overline{\beta}_r)}{d\lambda^2} \tag{2.12}$$

where $\delta\overline{\beta}_r = \delta\beta_r / k_0$. Combining (2.11) and (2.12), we obtain

$$\delta D = f(\lambda)D(\lambda) + \frac{\lambda}{c}\left[2\frac{df(\lambda)}{d\lambda}\frac{d\overline{\beta}(\lambda)}{d\lambda} + \frac{d^2 f(\lambda)}{d\lambda^2}\overline{\beta}(\lambda)\right] \tag{2.13}$$

where $D(\lambda)$ is the dispersion of the lossless fiber given by (2.5) and $f(\lambda)$ is defined as

$$f(\lambda) = -\frac{\lambda^2\alpha^2(\lambda)}{8\pi^2 n^2(\lambda)} \tag{2.14}$$

At $\lambda = 1.55\mu m$, the fiber attenuation in dB is $20\alpha\log_{10}e = 0.21\,\text{dB/km}$, and a typical fiber has $n = 1.458$. With these data, we obtain $\alpha = 0.02418$ 1/km and $f(\lambda)\big|_{\lambda=1.55\mu m} = 7.836\times10^{-24}$. It is Clear that δD is on the order of 10^{-20} ps/nm.km and thus can be neglected in all fibers of practical applications.

Chapter 3. Generalized Analysis of Multiple-Clad Optical Fibers

Optical fibers with two or more claddings are required for dispersion shifting, dispersion flattening, and other specialized applications. In this chapter, a generalized analysis of multiple-clad fibers is presented. The geometry considered here is limited to a four-layer cylindrical dielectric structure, consisting of a core and three claddings. A unified formulation is developed which is applicable to all possible triple-clad fibers with step-index profiles. Furthermore, by reducing one or two layers to zero, double-clad, and single-clad geometries are also covered by this formulation. Thus, the formulation presented in this chapter is applicable to optical fibers with one, two, and three claddings.

3.1 Geometry and Parameters

Let us consider a four-layer cylindrical dielectric structure as shown in Figure 3.1. All layers are assumed to be lossless, linear, isotropic, homogeneous, and nonmagnetic. A cylindrical coordinate system (r, ϕ, z), with the z-axis coinciding with the axis of the

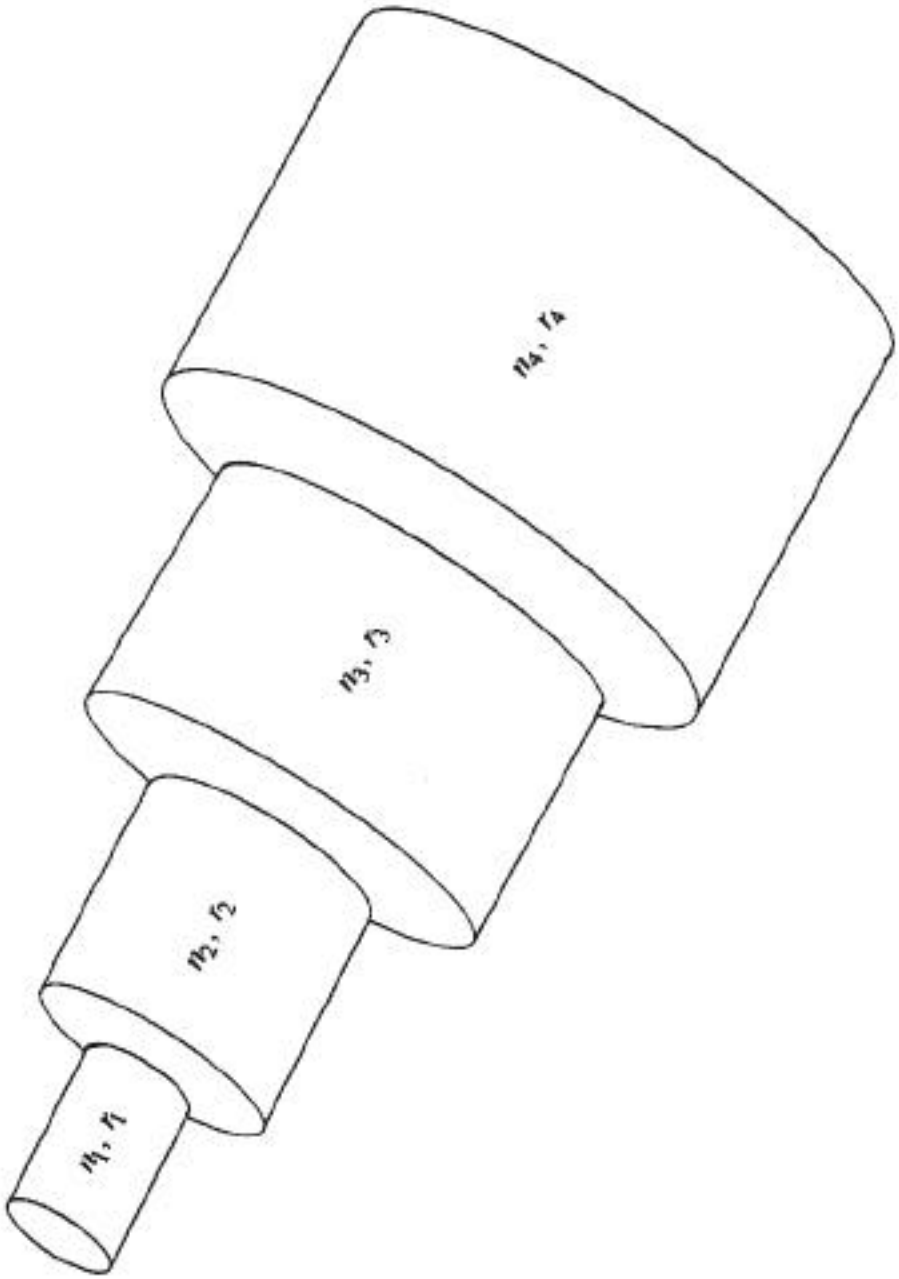

Figure 3.1 Geometry of triple-clad fiber.

dielectric structure, is chosen for the field analysis. The ith layer has a radius r_i and a refractive index n_i; $i = 1, 2, 3, 4$. $i = 1$ corresponds to the central core region, while $i = 2, 3,$ and 4 refer to cladding layers. The outer cladding layer ($i = 4$) is assumed to extend to infinity in the radial direction. This assumption is justified for guided modes whose fields decay exponentially in the radial direction.

The analysis presented in this chapter can accommodate a large variety of index profiles. These profiles are illustrated in Figures 3.2-3.4. The profiles shown in Figures 3.2 and 3.3 are all for triple-clad fibers, while the profiles in Figure 3.4a-3.4d are for double-clad and that in Figure 3.4e is for an ordinary single-clad fiber. Moreover, for the profiles in Figure 3.2, the central core region assumes the largest index, whereas for the profiles in Figure 3.3, one of the inner claddings has the largest refractive index. In the latter figure, not all possible cases are shown. It may be noted that a total of 18 different profile combinations for triple-clad fibers and five combinations for double-clad fibers exist. Thus, the formulation presented here is essentially applicable to 24 different profile configurations associated with fibers having one, two, or three claddings.

The index profile in Figure 3.4a may be considered as a special case of profiles in Figures 3.2f, 3.3c, and 3.3d in which r_1 approaches zero, the profile in Figure 3.2a in which $r_1 - r_2$ approaches zero, or the profile in Figure 3.2c in which $r_3 - r_2$ approaches zero. In a similar manner, other profiles in Figure 3.4 may be considered as special cases of one or more profiles of Figures 3.2 and 3.3.

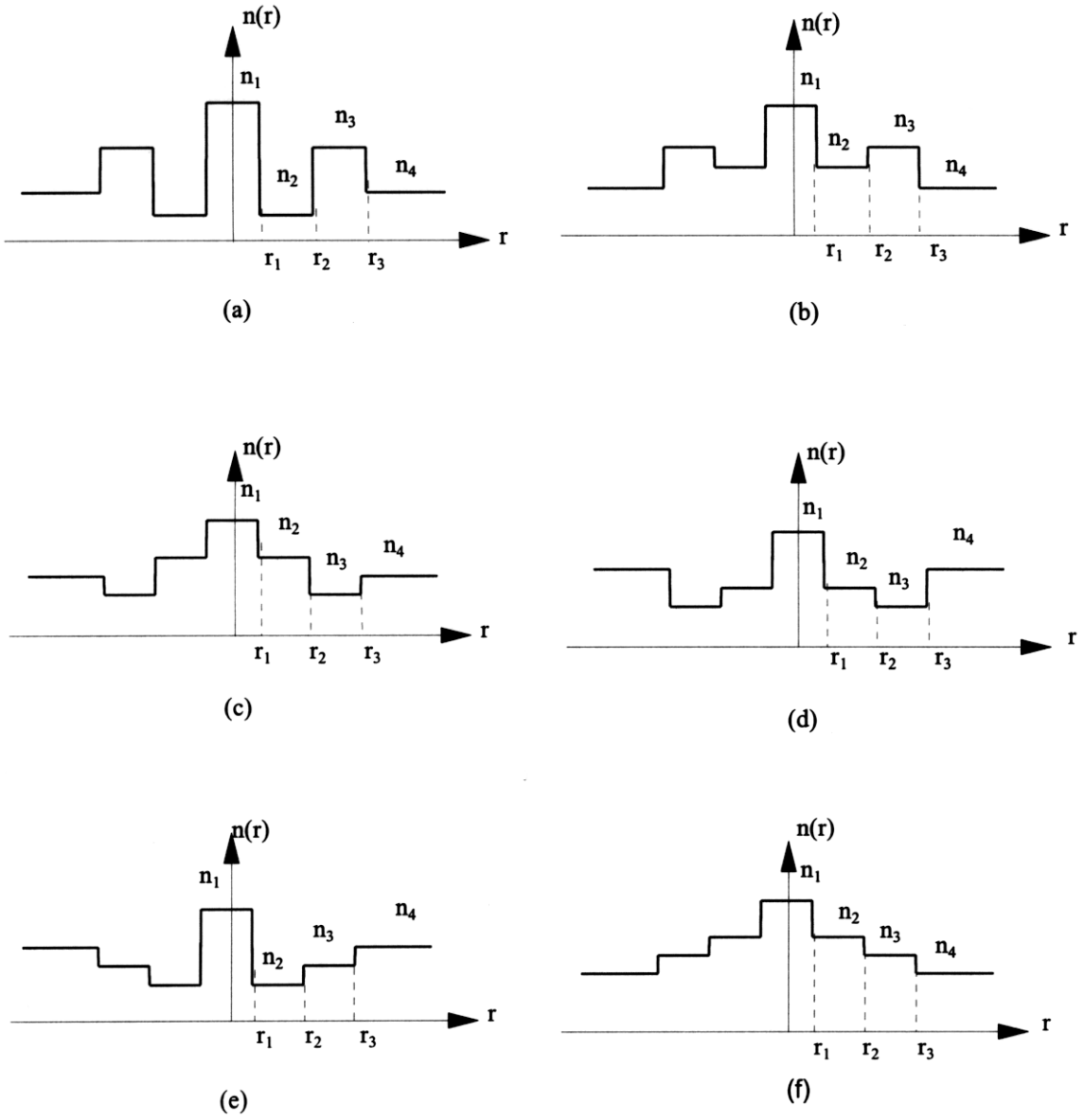

Figure 3.2. Index profiles for triple-clad fibers with core region having the largest refractive index.

(a) $n_2 \le n_4 < n_3 \le n_1$

(b) $n_4 \le n_2 < n_3 \le n_1$

(c) $n_3 < n_4 \le n_2 < n_1$

(d) $n_3 < n_2 \le n_4 \le n_1$

(e) $n_2 < n_3 < n_4 < n_1$

(f) $n_4 < n_3 < n_2 < n_1$

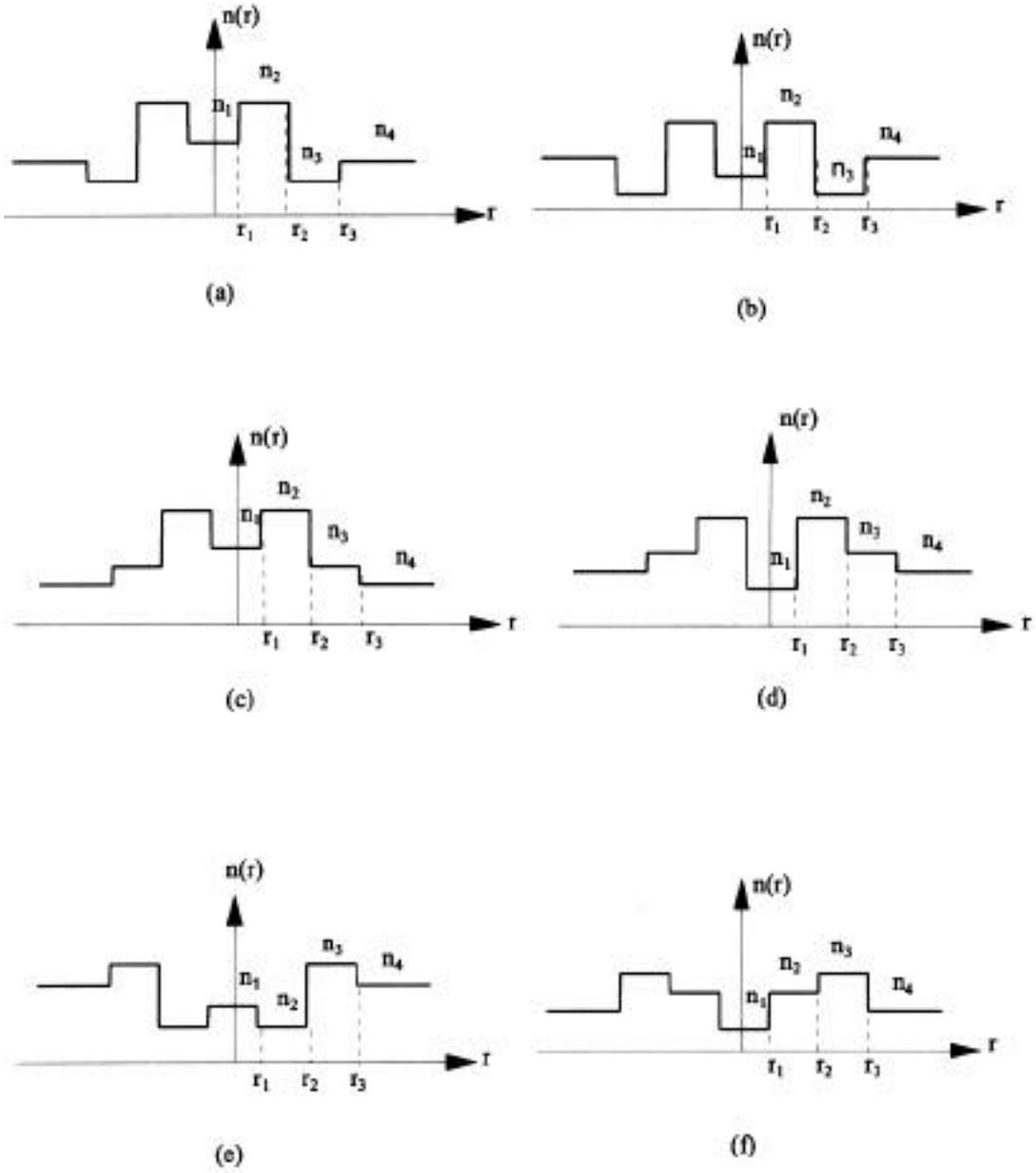

Figure 3.3. Index profiles for triple-clad fibers with one of the inner claddings having the largest refractive index.

(a) $n_3 < n_4 \le n_1 < n_2$

(b) $n_3 \le n_1 < n_4 \le n_2$

(c) $n_4 < n_3 \le n_1 < n_2$

(d) $n_1 < n_4 < n_3 < n_2$

(e) $n_2 < n_1 \le n_4 < n_3$

(f) $n_1 \le n_4 < n_2 < n_3$

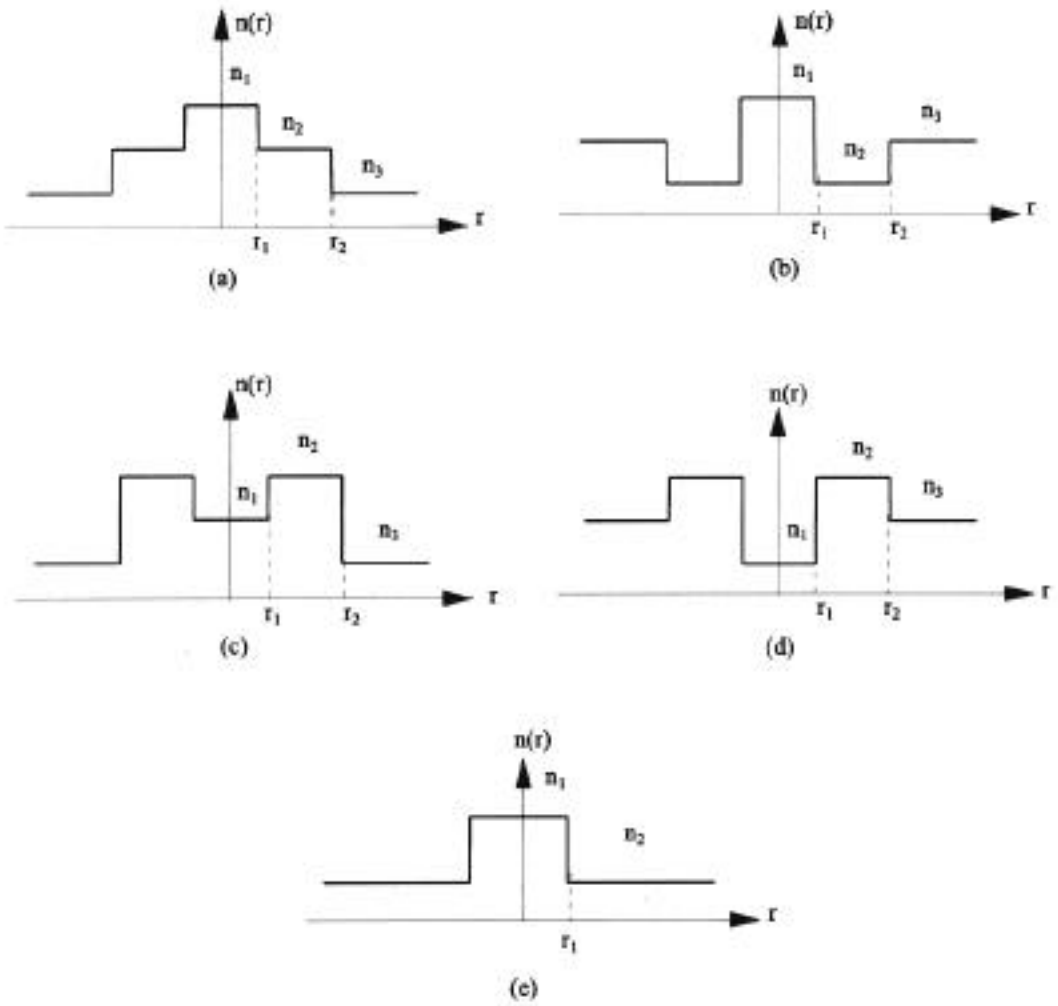

Figure 3.4. Index profiles for double-clad and single-clad fibers as special cases of triple-clad fibers.

(a) $n_3 < n_2 < n_1$

(b) $n_2 < n_3 < n_1$

(c) $n_3 \leq n_1 < n_2$

(d) $n_1 \leq n_3 < n_2$

(e) $n_2 < n_1$

3.2 Field Analysis

Electromagnetic fields in multiple clad fibers described in section 3.1 are solutions of Maxwell's equations subject to boundary conditions. In deriving these solutions, we focus attention on guided modes only and take advantage of weakly guiding conditions, which are always met for optical fibers of practical interest, in order to simplify the solutions. Weakly guiding conditions imply that the index difference between two neighboring layers is very small; that is, $\Delta_i = |(n_{i+1} - n_i)/\, n_i| << 1,\ i = 1,\ 2,\ 3$ for triple-clad fibers. These conditions allow a scalar-wave analysis to be employed [18]. Considering time-harmonic fields propagating in the positive z-direction, the time and z-dependencies of fields are as $e^{j(\omega t - \beta z)}$, where β is the axial propagation constant. This term, which is common to all field components, is dropped from the solutions.

3.2.1 Scalar Field Solutions

Scalar fields are solutions of the scalar wave equation expressed as

$$\nabla_t^2 \psi + (k_0^2 n^2 - \beta^2)\psi = 0 \tag{3.1}$$

where ψ is a Cartesian transverse component of electric or magnetic fields, ∇_t^2 is the transverse Laplacian operator, $k_0 = 2\pi / \lambda$ is the free space wave number, and n is the refractive index of the medium in which electromagnetic fields are sought. In the cylindrical coordinate system, (3.1) is written as

$$\frac{\partial^2 \psi}{\partial r^2} + \frac{1}{r}\frac{\partial \psi}{\partial r} + \frac{1}{r^2}\frac{\partial^2 \psi}{\partial \phi^2} + \bar{k}^2 \psi = 0 \tag{3.2}$$

where $\bar{k}^2 = k_0^2 n^2 - \beta^2$.

The solution of (3.2) is obtained by the method of separation of variables. Assuming that $\psi(r, \phi) = R(r)\Phi(\phi)$, (3.2) resolves into the following two ordinary differential equations:

$$\frac{d^2R}{dr^2}+\frac{1}{r}\frac{dR}{dr}+\left(\bar{k}^2-\frac{\upsilon^2}{r^2}\right)R=0 \tag{3.3}$$

$$\frac{d^2\Phi}{d\phi^2}+\upsilon^2\Phi=0 \tag{3.4}$$

where υ is a separation constant. The solution of (3.4) is readily obtained as

$$\Phi(\phi)=A_1\cos\upsilon\phi+B_1\sin\upsilon\phi \tag{3.5}$$

where A_1 and B_1 are constant coefficients. Since field solutions are periodic in ϕ, i.e. $\psi(\phi+2\pi)=\psi(\phi)$, it is necessary that υ be an integer. The integer υ can be determined once fiber parameters, frequency of operation, and excitation mechanism are known. Each $\cos\upsilon\phi$ and $\sin\upsilon\phi$ alone (and of course their linear combination as in (3.5)) may be used in the field solutions. In fact, $\cos\upsilon\phi$ and $\sin\upsilon\phi$ represent separate degenerate modes. Here, the ϕ-dependent part of the solutions is expressed as $\begin{pmatrix}\cos\upsilon\phi\\ \sin\upsilon\phi\end{pmatrix}$.

Equation (3.3) is recognized as the Bessel differential equation with the following solutions

$$R(r)=\begin{cases}A_2J_\upsilon(\bar{k}r)+B_2Y_\upsilon(\bar{k}r), & \bar{k}^2>0\\ A_3I_\upsilon(|\bar{k}|r)+B_3K_\upsilon(|\bar{k}|r), & \bar{k}^2<0\end{cases} \tag{3.6}$$

Where J_n and Y_n, are the Bessel functions of the first and second kinds, while I_n and K_n are the modified Bessel functions of the first and second kinds, respectively. In these solutions A_2, A_3, B_2, and B_3 are constant amplitude coefficients. In the central layer, i.e. in the core region, Y_υ and K_υ must be discarded, because these functions are undefined at $r=0$ (Note that the core region is defined as $0\le r\le r_1$). In the outer cladding layer, $r\ge r_3$, the field of guided modes must decay exponentially in the radial direction. This behavior is maintained by the K_υ function only. Thus, in the outer cladding $R(r)$ is proportional to

$K_\upsilon(|k_4|r)$. In the inner cladding layers, both Bessel functions J_υ and Y_υ or modified Bessel Functions I_υ and K_υ are needed. The choice of Bessel or modified Bessel functions in all but the outer layer region is determined by the sign of $\bar{k}^2$. The sign of $\bar{k}^2$, in turn, is determined by realizing that for guided modes $k_0 n_4 < \beta < k_0 n_{\max}$, where $n_{\max}$ is the highest index in the profile. For example, for the profile in Figure 3.2a with $n_2 < n_4 < n_3 \le n_1$, fields in the central layer ($0 \le r \le r_1$) involve only the J_υ function, while fields in the first inner cladding ($r_1 \le r \le r_2$) involve I_υ and K_υ functions. However, in the second cladding region ($r_2 \le r \le r_3$), if $k_0 n_3 < \beta < k_0 n_1$ fields involve I_υ and K_υ functions, whereas for $k_0 n_4 < \beta < k_0 n_3$ fields are expressed in terms of J_υ and Y_υ functions.

3.2.2 Generalized Field Solutions

Based on the above mentioned considerations on the choice of Bessel or modified Bessel functions, generalized scalar field solutions are written as

$$\psi(r,\phi) = \begin{cases} \psi_1(r,\phi) = AZ_{n1}(k_1 r)Q(\phi), & 0 \le r \le r_1 \\ \psi_2(r,\phi) = \left[BZ_{n2}(k_2 r) + C\bar{Z}_{n2}(k_2 r)\right]Q(\phi), & r_1 \le r \le r_2 \\ \psi_3(r,\phi) = \left[DZ_{n3}(k_3 r) + E\bar{Z}_{n3}(k_3 r)\right]Q(\phi), & r_2 \le r \le r_3 \\ \psi_4(r,\phi) = FZ_{n4}(k_4 r)Q(\phi), & r \ge r_3 \end{cases} \tag{3.7}$$

where

$$Q(\phi) = \begin{pmatrix} \cos\upsilon\phi \\ \sin\upsilon\phi \end{pmatrix} \tag{3.8}$$

$$k_i = \left[\kappa_i(\beta^2 - k_0^2 n_i^2)\right]^{1/2},\ i = 1,...,4 \tag{3.9}$$

with

$$\kappa_i = \begin{cases} +1, & \text{if } \beta > k_0 n_i \\ -1, & \text{if } \beta < k_0 n_i \end{cases}, \quad i = 1,...,4 \tag{3.10}$$

The functions Z_{ni}, $i = 1,...,4$, and $\overline{Z}_{ni}$, $i = 1,2,3$, are defined in Table 3.1

3.2.3 Boundary Conditions

In dielectric waveguides, boundary conditions require the continuity of tangential field components at different interfaces. In weakly guiding fibers, scalar-wave analysis introduces great simplifications by approximating the exact boundary conditions to the continuity of $\psi(r,\phi)$ and $\partial\psi(r,\phi)/\partial r$. This approximation reduces the number of boundary conditions for a triple-clad optical fiber from 12 to a set of six homogeneous equations. These approximations have been proven to be very accurate for weakly guiding optical fibers [18]. The expression for $\partial\psi(r,\phi)/\partial r$ is first obtained from (3.7), then boundary conditions are applied at different interfaces as follows

Table 3.1 Definitions of functions Z_{ni}, $i = 1,...,4$, and $\overline{Z}_{ni}$, $i = 2,3$.

Z_{n1}	$\kappa_1 = 1$ $\kappa_1 = -1$	I_υ J_υ
Z_{n2}	$\kappa_2 = 1$ $\kappa_2 = -1$	I_υ J_υ
$\overline{Z}_{n2}$	$\kappa_2 = 1$ $\kappa_2 = -1$	K_υ Y_υ
Z_{n3}	$\kappa_3 = 1$ $\kappa_3 = -1$	I_υ J_υ
$\overline{Z}_{n3}$	$\kappa_3 = 1$ $\kappa_3 = -1$	K_υ Y_υ
Z_{n4}	$\kappa_4 = 1$	K_υ

$$\frac{\partial \psi(r,\phi)}{\partial r} = \begin{cases} \dfrac{\partial \psi_1(r,\phi)}{\partial r} = Ak_1 Z_{n1}'(k_1 r) Q(\phi), & 0 \le r \le r_1 \\ \dfrac{\partial \psi_2(r,\phi)}{\partial r} = \left[BZ_{n2}'(k_2 r) + C\bar{Z}_{n2}'(k_2 r) \right] k_2 Q(\phi), & r_1 \le r \le r_2 \\ \dfrac{\partial \psi_3(r,\phi)}{\partial r} = \left[DZ_{n3}'(k_3 r) + E\bar{Z}_{n3}'(k_3 r) \right] k_3 Q(\phi), & r_2 \le r \le r_3 \\ \dfrac{\partial \psi_4(r,\phi)}{\partial r} = Fk_4 Z_{n4}'(k_4 r) Q(\phi), & r \ge r_3 \end{cases} \tag{3.11}$$

where the prime sign indicates differentiation with respect to the argument of Z_{ni} or $\bar{Z}_{ni}$ functions.

At $r = r_1$, $\psi_1(r_1,\phi) = \psi_2(r_1,\phi)$ and $\left.\frac{\partial \psi_1(r,\phi)}{\partial r}\right|_{r=r_1} = \left.\frac{\partial \psi_2(r,\phi)}{\partial r}\right|_{r=r_1}$ yield

$$AZ_{n1}(k_1 r_1) = BZ_{n2}(k_2 r_1) + C\bar{Z}_{n2}(k_2 r_1) \tag{3.12}$$

$$Ak_1 Z_{n1}'(k_1 r_1) = \left[BZ_{n2}'(k_2 r_1) + C\bar{Z}_{n2}'(k_2 r_1) \right] k_2 \tag{3.13}$$

Similarly, at $r = r_2$, $\psi_2(r_2,\phi) = \psi_3(r_2,\phi)$ and $\left.\frac{\partial \psi_2(r,\phi)}{\partial r}\right|_{r=r_2} = \left.\frac{\partial \psi_3(r,\phi)}{\partial r}\right|_{r=r_2}$ result in

$$BZ_{n2}(k_2 r_2) + C\bar{Z}_{n2}(k_2 r_2) = DZ_{n3}(k_3 r_2) + E\bar{Z}_{n3}(k_3 r_2) \tag{3.14}$$

$$\left[BZ_{n2}'(k_2 r_2) + C\bar{Z}_{n2}'(k_2 r_2) \right] k_2 = \left[DZ_{n3}'(k_3 r_2) + E\bar{Z}_{n3}'(k_3 r_2) \right] k_3 \tag{3.15}$$

Finally, at $r = r_3$, $\psi_3(r_3,\phi) = \psi_4(r_3,\phi)$ and $\left.\frac{\partial \psi_3(r,\phi)}{\partial r}\right|_{r=r_3} = \left.\frac{\partial \psi_4(r,\phi)}{\partial r}\right|_{r=r_3}$ give

$$DZ_{n3}(k_3 r_3) + E\bar{Z}_{n3}(k_3 r_3) = FZ_{n4}(k_4 r_3) \tag{3.16}$$

$$\left[DZ_{n3}'(k_3 r_3) + E\bar{Z}_{n3}'(k_3 r_3) \right] k_3 = Fk_4 Z_{n4}'(k_4 r_3) \tag{3.17}$$

Equations (3.12) to (3.17) may be written in a matrix form as

$$\left[a_{ij}\right]\begin{bmatrix} A \\ B \\ C \\ D \\ E \\ F \end{bmatrix} = 0 \quad i = 1,2,...,6 \text{, and } j = 1,2,...,6 \tag{3.18}$$

where $\left[a_{ij}\right]$ is a 6×6 matrix given in (3.19). The determinant of this matrix defines the dispersion relation.

$$\left[a_{ij}\right] = \begin{bmatrix} Z_{n1}(k_1r_1) & -Z_{n2}(k_2r_1) & -\bar{Z}_{n2}(k_2r_1) & 0 & 0 & 0 \\ k_1Z'_{n1}(k_1r_1) & -k_2Z'_{n2}(k_2r_1) & -k_2\bar{Z}'_{n2}(k_2r_1) & 0 & 0 & 0 \\ 0 & Z_{n2}(k_2r_2) & \bar{Z}_{n2}(k_2r_2) & -Z_{n3}(k_3r_2) & -\bar{Z}_{n3}(k_3r_2) & 0 \\ 0 & k_2Z'_{n2}(k_2r_2) & k_2\bar{Z}'_{n2}(k_2r_2) & -k_3Z'_{n3}(k_3r_2) & -k_3\bar{Z}'_{n3}(k_3r_2) & 0 \\ 0 & 0 & 0 & Z_{n3}(k_3r_3) & \bar{Z}_{n3}(k_3r_3) & -Z_{n4}(k_4r_3) \\ 0 & 0 & 0 & k_3Z'_{n3}(k_3r_3) & k_3\bar{Z}'_{n3}(k_3r_3) & -k_4Z'_{n4}(k_4r_3) \end{bmatrix} \tag{3.19}$$

For equations (3.12) to (3.17) to have nontrivial solutions, the determinant of the coefficients, i.e. $\left|a_{ij}\right|$ must vanish. The condition $\left|a_{ij}\right| = 0$ is, in fact, the characteristic equation (also known as dispersion equation and eigenvalue equation) from which the propagation constant β is determined.

3.2.4 Amplitude Coefficients

The fact that six equations resulting from the boundary conditions constitute a homogeneous set implies that only five of the six equations are independent of each other, and the sixth one can always be obtained from a linear combination of the rest in conjunction with the characteristic equation. Thus, any five equations may solved for five coefficients in terms of a sixth one. For example, B, C, D, E and F, may be calculated in terms of A. First we solve (3.12) and (3.13) for B and C. Then (3.15) and (3.16) are solved for D and E. Finally F is obtained from (3.16). Doing so, we obtain

$$B = \frac{Z_{n1}(X_1)}{Z_{n2}(X_2)} \frac{\eta_1 - \eta_3}{\eta_2 - \eta_3} A \tag{3.20}$$

$$C = \frac{Z_{n1}(X_1)}{\overline{Z}_{n2}(X_2)} \frac{\eta_1 - \eta_2}{\eta_3 - \eta_2} A \tag{3.21}$$

$$D = \frac{Z_{n2}(\overline{X}_2)}{Z_{n3}(X_3)} \frac{\eta_7 - \eta_4}{\eta_7 - \eta_6} B + \frac{\overline{Z}_{n2}(\overline{X}_2)}{Z_{n3}(X_3)} \frac{\eta_7 - \eta_5}{\eta_7 - \eta_6} C \tag{3.22}$$

$$E = \frac{Z_{n2}(\overline{X}_2)}{\overline{Z}_{n3}(X_3)} \frac{\eta_6 - \eta_4}{\eta_6 - \eta_7} B + \frac{\overline{Z}_{n2}(\overline{X}_2)}{\overline{Z}_{n3}(X_3)} \frac{\eta_6 - \eta_5}{\eta_6 - \eta_7} C \tag{3.23}$$

$$F = \frac{Z_{n3}(\overline{X}_3)}{Z_{n4}(X_4)} D + \frac{\overline{Z}_{n3}(\overline{X}_3)}{Z_{n4}(X_4)} E \tag{3.24}$$

where

$$\eta_1 = \frac{X_1 Z'_{n1}(X_1)}{Z_{n1}(X_1)} \tag{3.25}$$

$$\eta_2 = \frac{X_2 Z'_{n2}(X_2)}{Z_{n2}(X_2)} \tag{3.26}$$

$$\eta_3 = \frac{X_2 \overline{Z}'_{n2}(X_2)}{\overline{Z}_{n2}(X_2)} \tag{3.27}$$

$$\eta_4 = \frac{\overline{X}_2 Z'_{n2}(\overline{X}_2)}{Z_{n2}(\overline{X}_2)} \tag{3.28}$$

$$\eta_5 = \frac{\overline{X}_2 \overline{Z}'_{n2}(\overline{X}_2)}{\overline{Z}_{n2}(\overline{X}_2)} \tag{3.29}$$

$$\eta_6 = \frac{X_3 Z'_{n3}(X_3)}{Z_{n3}(X_3)} \tag{3.30}$$

$$\eta_7 = \frac{X_3 \overline{Z}'_{n3}(X_3)}{\overline{Z}_{n3}(X_3)} \tag{3.31}$$

with

$$X_1 = k_1 r_1 \tag{3.32}$$

$$X_2 = k_2 r_1 \tag{3.33}$$

$$\overline{X}_2 = k_2 r_2 \tag{3.34}$$

$$X_3 = k_3 r_2 \tag{3.35}$$

$$\overline{X}_3 = k_3 r_3 \tag{3.36}$$

$$X_4 = k_4 r_4 \tag{3.37}$$

Substituting equations (3.20) and (3.21) into (3.22), (3.23), and (3.24) respectively, coefficients D, E, and F are expressed solely in terms of A.

In determining radial field distributions, the coefficient A is set equal to unity. Then all the remaining amplitude coefficients can be calculated once fiber parameters and its material compositions, the wavelength of operation and the mode to be studied are known.

3.3 Characteristic Equation

To obtain a simplified expression of the characteristic equation, equations (3.20), (3.16), and (3.22) are divided by (3.21), (3.17), and (3.23) respectively, yielding the following results

$$\frac{B}{C} = -\frac{\bar{Z}_{n2}(X_2)}{Z_{n2}(X_2)}\frac{\eta_1 - \eta_3}{\eta_1 - \eta_2} \tag{3.38}$$

$$\frac{D}{E} = -\frac{\bar{Z}_{n3}(\bar{X}_3)}{Z_{n3}(\bar{X}_3)}\frac{\eta_{10} - \eta_9}{\eta_{10} - \eta_8} \tag{3.39}$$

$$\frac{D}{E} = -\frac{\bar{Z}_{n3}(X_3)}{Z_{n3}(X_3)}\frac{(\eta_7 - \eta_4)\frac{B}{C} + \frac{\bar{Z}_{n2}(\bar{X}_2)}{Z_{n2}(\bar{X}_2)}(\eta_7 - \eta_5)}{(\eta_6 - \eta_4)\frac{B}{C} + \frac{\bar{Z}_{n2}(\bar{X}_2)}{Z_{n2}(\bar{X}_2)}(\eta_6 - \eta_5)} \tag{3.40}$$

where

$$\eta_8 = \frac{\bar{X}_3 Z'_{n3}(\bar{X}_3)}{Z_{n3}(\bar{X}_3)} \tag{3.41}$$

$$\eta_9 = \frac{\bar{X}_3 \bar{Z}'_{n3}(\bar{X}_3)}{\bar{Z}_{n3}(\bar{X}_3)} \tag{3.42}$$

$$\eta_{10} = \frac{X_4 Z'_{n4}(X_4)}{Z_{n4}(X_4)} \tag{3.43}$$

Substituting for D/E and B/C, from (3.38) and (3.39) into (3.40) yields an equation, known as the characteristic equation, dispersion equation, or eigenvalue equation.

$$\xi_2 \frac{\eta_{10} - \eta_9}{\eta_{10} - \eta_8} = \frac{(\eta_1 - \eta_3)(\eta_4 - \eta_7) - \xi_1(\eta_1 - \eta_2)(\eta_5 - \eta_7)}{(\eta_1 - \eta_3)(\eta_4 - \eta_6) - \xi_1(\eta_1 - \eta_2)(\eta_5 - \eta_6)} \tag{3.44}$$

where

$$\xi_1 = \frac{\bar{Z}_{n2}(\bar{X}_2) Z_{n2}(X_2)}{\bar{Z}_{n2}(X_2) Z_{n2}(\bar{X}_2)} \tag{3.45}$$

$$\xi_2 = \frac{\bar{Z}_{n3}(\bar{X}_3) Z_{n3}(X_3)}{\bar{Z}_{n3}(X_3) Z_{n3}(\bar{X}_3)} \tag{3.46}$$

The characteristic equation is a function of fiber parameters, including radii of different layers and their refractive indices, the azimuthal number υ, the wavelength of light λ, and the propagation constant β. It may be expressed as

$$f(r_i, n_i; i = 1,..., 4, \upsilon, \lambda, \beta) = 0 \tag{3.47}$$

For a given fiber with specified parameters, and some value of υ, (3.47) becomes only a function of λ and β. This equation is usually transcendental and should be solved numerically. The numerical solution of the characteristic equation is addressed in Chapter 4. For a given wavelength, given fiber parameters, and a specified value of υ, there may be several solutions for β each representing a guided mode. These modes are designated as $LP_{\upsilon m}$, where LP signifies the "Linearly Polarized" character of the modes in weakly guiding fibers. The integer parameter $m \geq 1$ is the order of the mode and may be attributed to field maxima/minima in the radial direction. On the other hand, the integer $\upsilon \geq 0$ is related to field maxima/minima in the azimuthal direction.

3.4 Cutoff Conditions

As mentioned earlier in this chapter, the normalized propagation constant for guided modes in a multi-clad cylindrical optical waveguide should always be bounded by the refractive index of the outermost layer of the guide on one end, and by the largest refractive index in the profile studied, i.e. $n_4 < \bar{\beta} < n_{\max}$. Cutoff occurs when $\bar{\beta} = n_4$ or, in other words, when $k_4 = 0$. Thus, cutoff conditions can be determined from the characteristic equation in the limit of k_4 approaching zero. Since η_{10} is the only term that is a function of k_4, its limit as $k_4 \to 0$ is derived first using the small argument approximation of $Z_{n4}(X_4) = K_\upsilon(X_4)$,

$$Z_{n4}(X_4) \xrightarrow[X_4 \to 0]{} \begin{cases} \ln\left(\frac{2}{\gamma X_4}\right), & \upsilon = 0 \\ \frac{1}{2}(\upsilon - 1)!\left(\frac{2}{X_4}\right)^{\upsilon}, & \upsilon \geq 1 \end{cases} \tag{3.48}$$

Thus,

$$\eta_{10} = \frac{X_4 Z'_{n4}(X_4)}{Z_{n4}(X_4)} = \frac{-X_4 K_{\upsilon-1}(X_4)}{K_\upsilon(X_4)} - \upsilon \tag{3.49}$$

and

$$\eta_{10} \xrightarrow[X_4 \to 0]{} \begin{cases} 0, & \upsilon = 0 \\ -\upsilon, & \upsilon \geq 1 \end{cases} \tag{3.50}$$

where $\gamma = .5772156649...$ is Euler's constant. Substituting (3.50) in the characteristic equation yields an equation from which cutoff frequencies for all modes are obtained.

$$\xi_2 \frac{\upsilon + \eta_9}{\upsilon + \eta_8} = \frac{(\eta_1 - \eta_3)(\eta_4 - \eta_7) - \xi_1(\eta_1 - \eta_2)(\eta_5 - \eta_7)}{(\eta_1 - \eta_3)(\eta_4 - \eta_6) - \xi_1(\eta_1 - \eta_2)(\eta_5 - \eta_6)} \tag{3.51}$$

with $\bar{\beta} = n_4$. For most dielectric waveguides, the cutoff frequency of the fundamental LP_{01} mode is zero. However, under certain circumstances and for certain waveguides, LP_{01} mode may have a non-zero cutoff. The cutoff of the LP_{01} mode , if exists, is obtained from (3.51) with $\upsilon = 0$. The condition under which the LP_{01} mode exhibits a non-zero cutoff may be obtained by examining (3.51) in the limit of $\omega \to 0$ and $\bar{\beta} \to n_4$. Deriving a generalized condition for the non-zero cutoff of the LP_{01} mode is very involved. So, for the sake of simplicity, the special case of a triple-clad fiber with the first cladding region having the highest refractive index in the profile is examined as an example case.

For zero cutoff, $\omega = 0$ and $\bar{\beta} = n_4$ must satisfy the characteristic equation. As the angular frequency ω nears zero, the arguments of all the Bessel and modified Bessel functions become very small, and small argument approximations for all η's as well as ξ_1 and ξ_2 are needed. Using the small argument approximations of the Bessel and modified Bessel functions given in the appendix, the corresponding approximations for η's, ξ_1 and ξ_2 are obtained as summarized in Table 3.2. Using these approximations in the characteristic equation, yields

Table 3.2 Small arguments approximations for η_i, $i = 1,...,9$, and ξ_1 and ξ_2.

$\eta_1 \to \frac{1}{2} X_1^2$	$\eta_2 \to -\frac{1}{2} X_2^2$	$\eta_3 \to \frac{1}{\ln X_2}$	$\eta_4 \to -\frac{1}{2} \overline{X}_2^2$
$\eta_5 \to \frac{1}{\ln \overline{X}_2}$	$\eta_6 \to \frac{1}{2} X_3^2$	$\eta_7 \to \frac{1}{\ln X_3}$	$\eta_8 \to \frac{1}{2} \overline{X}_3^2$
$\eta_9 \to \frac{1}{\ln \overline{X}_3}$	$\eta_{10} \to \frac{1}{\ln X_4}$	$\xi_1 \to 1$	$\xi_2 \to 1$

$$\frac{1}{\ln X_4} = \frac{1}{2}\left[X_1^2 + X_2^2 + \overline{X}_3^2 - \overline{X}_2^2 - X_3^2\right] \tag{3.52}$$

Since the left side of this equation is always negative, the condition for zero cutoff of the LP_{01} mode reduces to requiring the right side of (3.52) to be negative too. Conversely, the condition for non-zero cutoff is met whenever the right side of equation (3.52) is positive. That is

$$X_1^2 + X_2^2 + \overline{X}_3^2 - \overline{X}_2^2 - X_3^2 > 0 \tag{3.53}$$

or

$$\frac{X_1^2 + X_2^2 + \overline{X}_3^2}{\overline{X}_2^2 - X_3^2} > 1 \tag{3.54}$$

Substituting for X_1, X_2, $\overline{X}_2$, X_3, and $\overline{X}_3$ from equations (3.32) to (3.36) respectively, we obtain

$$\frac{(n_4^2 - n_1^2) r_1^2 + (n_2^2 - n_4^2) r_2^2 + (n_4^2 - n_3^2) r_3^2}{(n_2^2 - n_4^2) r_2^2 + (n_4^2 - n_3^2) r_2^2} > 1 \tag{3.55}$$

Rearranging the terms, (3.55) is written as

$$\left(\frac{n_2^2 - n_1^2}{n_2^2 - n_3^2}\frac{r_1}{r_2}\right)^2 + \left(\frac{n_4^2 - n_3^2}{n_2^2 - n_3^2}\frac{r_3}{r_2}\right)^2 > 1. \tag{3.56}$$

Defining refractive index differences Δ_1, Δ_3, Δ_4, and Δ_3'

$$\Delta_1 = \frac{n_2^2 - n_1^2}{2n_2^2}, \tag{3.57}$$

$$\Delta_3 = \frac{n_2^2 - n_3^2}{2n_2^2}, \tag{3.58}$$

$$\Delta_4 = \frac{n_2^2 - n_4^2}{2n_2^2}, \tag{3.59}$$

$$\Delta_3' = \Delta_3 - \Delta_4, \tag{3.60}$$

the condition for non-zero cutoff of the LP_{01} mode is expressed as

$$\Delta_1 \left(\frac{r_1}{r_2}\right)^2 + \Delta_3' \left(\frac{r_3}{r_2}\right)^2 > \Delta_3. \tag{3.61}$$

The relationship in (3.61) may be used to design optical fibers whose fundamental mode exhibits a non-zero cutoff frequency. Such fibers may find applications in dispersion compensation for upgrading the $1.3\mu m$ link for operation at the $1.55\mu m$ wavelength.

Chapter 4. Numerical Results

The formulation developed in Chapter 3 is used to design and analyze several single-mode fibers with triple-clad geometries. Four design examples for conventional dispersion-shifted fiber, dispersion-flattened fiber, dispersion compensating fiber, and optimized dispersion-shifted fiber are presented. Transmission properties including normalized propagation constant, dispersion characteristics, cutoff wavelengths, and radial field distributions, are evaluated. Numerical results, illustrating variations of propagation constant and dispersion versus wavelength are presented for the lower order modes. Also, plots of radial field distributions at $\lambda = 1.55 \mu m$ are provided.

4.1 Calculation of Transmission Properties

A computer program was developed for the numerical solution of the dispersion equation (3.55). The input data to this program include material compositions and radii of various layers of the waveguide, the wavelength, and the mode numbers for the desired mode. A listing of silica-based materials, commonly used in optical fiber fabrication, is provided in Table 4.1. The Sellmeier coefficients of the materials are stored in the program and are used for specified materials to calculate the refractive indices. Material compositions and parameters for four different fibers examined here are summarized in Table 4.2. The propagation constant is calculated as function of wavelength using a root search technique. For the materials of Table 4.1, it can be easily verified that the refractive indices vary slightly

Table 4.1 Material compositions of silica-based glasses.

Material	Composition
M1	Pure Silica
M2	13.5 m/o GeO_2 + 86.5 m/o SiO_2
M3	7.0 m/o GeO_2 +93.0 m/o SiO_2
M4	4.1 m/o GeO_2 , 95.9 m/o SiO_2
M5	9.1 m/o GeO_2 , 7.7 m/o B_2O_3 , 83.2 m/o SiO_2
M6	4.03 m/o GeO_2 , 9.7 m/o B_2O_3 , 86.27 m/o SiO_2
M7	0.1 m/o GeO_2 , 5.4 m/o B_2O_3 , 94.5 m/o SiO_2
M8	13.5 m/o B_2O_3 , 86.5 m/o SiO_2
M9	13.5 m/o B_2O_3 , 86.5 m/o SiO_2 (Chilled)
M10	3.1 m/o GeO_2 , 96.9 m/o SiO_2
M11	3.5 m/o GeO_2 , 96.5 m/o SiO_2
M12	5.8 m/o GeO_2 , 94.2 m/o SiO_2
M13	7.9 m/o GeO_2 , 92.1 m/o SiO_2
M14	3.0 m/o B_2O_2 , 97.0 m/o SiO_2
M15	3.5 m/o B_2O_2 , 96.5 m/o SiO_2
M16	3.3 m/o GeO_2 , 9.2 m/o B_2O_3 , 87.5 m/o SiO_2
M17	2.2 m/o GeO_2 , 3.3 m/o B_2O_3 , 94.5 m/o SiO_2
M18	Quenched Silica
M19	13.5m/o GeO_2 , 86.5 m/o SiO_2
M20	9.1 m/o P_2O_5 , 90.9 m/o SiO_2
M21	13.3 m/o B_2O_3 , 86.7 m/o SiO_2
M22	1.0 m/o F , 99.0 m/o SiO_2
M23	16.9 m/o Na_2O , 32.5 m/o B_2O_3 , 50.6 m/o SiO_2

Table 4.2 Parameters and material compositions for the designed fibers.

Fiber	Core	Clad 1	Clad 2	Clad 3
Fiber 1	M13 $r_1 = 3.2\mu m$	M1 $r_2 = 3.8\mu m$	M6 $r_3 = 4.3\mu m$	M4 $r_4 = \infty$
Fiber 2	M20 $r_1 = 2.9\mu m$	M8 $r_2 = 3.5\mu m$	M18 $r_3 = 4.5\mu m$	M4 $r_4 = \infty$
Fiber 3	M22 $r_1 = 5.3\mu m$	M23 $r_2 = 6.0\mu m$	M22 $r_3 = 7.4\mu m$	M20 $r_4 = \infty$
Fiber 4	M8 $r_1 = .2\mu m$	M2 $r_2 = 2.5\mu m$	M7 $r_3 = 5.3\mu m$	M5 $r_4 = \infty$

from one material to another, hence scalar field analysis is justified as discussed earlier in section 3.2. Let the normalized propagation constant, denoted as b, be defined as

$$b = \frac{\bar{\beta}^2 - n_4^2}{n_{\max}^2 - n_4^2} \tag{4.1}$$

where $n_{\max}$ is the highest refractive index in the profile of the chosen fiber under investigation. The importance of this definition for normalized propagation constant is that since $n_4 < \bar{\beta} < n_{\max}$, b always varies between 0 and 1, irrespective of the profile shape. The characteristic equation (3.55) is expressed as

$$f(\lambda, b) = f_1(\lambda, b) - f_2(\lambda, b) = 0 \tag{4.2}$$

where f_1 and f_2 represent the left-hand and right-hand sides of (3.55), respectively.

For a given fiber and at a specified wavelength, (4.2) is numerically solved for b. The wavelength is varied over the range $1.0\mu m$ to $1.7\mu m$ which corresponds to the low attenuation range for silica-based glass fibers. Dispersion is obtained by twice differentiating $\bar{\beta}$ with respect to wavelength, then substituting the results in equation (2.5) for the mode of interest. Plots of dispersion versus wavelength are then provided.

The radial field distribution is obtained from (3.7) at a specific wavelength for a given mode in a given fiber. Here, Field distributions are given for the LP_{01} mode at

$\lambda = 1.55 \mu m$. Normalized field distributions are plotted versus radial coordinate r. Polynomial approximations of the Bessel and modified Bessel functions of the first and second kinds, summarized in the Appendix, are used in the computations.

4.1.1 Dispersion Analysis

A. Dispersion-Shifted Design

The triple-clad geometry can be used to design a conventional dispersion-shifted fiber. An example of this design is fiber 1 with a refractive index profile such that $n_1 > n_4 > n_3 > n_2$. Figure 4.1 illustrates variations of the normalized propagation constant b versus wavelength for the two lowest order modes. It is noted that cutoff for the fundamental LP_{01} mode occurs at a wavelength $\lambda > 2 \mu m$, while the cutoff of the LP_{11} mode occurs at $0.96 \mu m$. All other modes have cutoff frequencies at lower wavelengths than that of the LP_{11} mode. Hence, fiber 1 is a single-mode waveguide over the entire range of wavelength $1.0 \mu m < \lambda < 2.0 \mu m$. Variations of dispersion versus wavelength for fiber 1 are shown in Figure 4.2. At the wavelength $\lambda = 1.55 \mu m$, this fiber exhibits a total dispersion less than $0.04 ps / nm.km$ and rate of change or slope of D is about $0.033 ps / nm^2.km$.

B. Dispersion-Flattened Design

Fiber 2 has been designed to provide a flattened dispersion characteristic. It has a refractive index profile such as that featured in Figure 3.2e with $n_1 > n_4 > n_3 > n_2$. Variations of normalized propagation constant versus wavelength for the LP_{01} and LP_{11} modes are shown in Figure 4.3. With all modes but the LP_{01} in cutoff over the range $0.99 \mu m < \lambda < 1.9 \mu m$, fiber 2 is strictly single-mode over this range of wavelengths. It is observed from Figure 4.4 that this fiber exhibits a total dispersion of less than $1 ps / nm.km$

over the range $1.38\mu m < \lambda < 1.59\mu m$. Furthermore, total dispersion vanishes at two wavelengths; namely at $\lambda = 1.42\mu m$ and $\lambda = 1.55\mu m$. The dispersion slopes at these two wavelengths are 0.0177 $ps / nm^2.km$ and -0.0176 $ps / nm^2.km$, respectively. These slopes, which are related to third-order dispersion, determine the amount of signal distortion if the fiber is operated at the above two wavelengths.

C. Dispersion Compensating Design

Next, the index profile of the triple-clad structure is tailored such that a large negative dispersion at $\lambda = 1.55\mu m$ is achieved. Fiber 3 is an example of a dispersion compensating fiber with a refractive index profile as that shown in Figure 3.3b. An important difference between the profile of this fiber and those of fibers 1 and 2 is that the first cladding and not the core assumes the largest refractive index. The propagation characteristics of few lower-order modes of this fiber are shown in Figure 4.5. It is noted that the cutoff wavelengths for the first three modes, LP_{01}, LP_{11}, and LP_{21}, are $1.6\mu m$, $1.53\mu m$, and $1.41\mu m$, respectively. Hence, fiber 3 may be used for single-mode transmission only over the narrow range of wavelengths $1.53\mu m < \lambda < 1.6\mu m$. The dispersion curve for the fundamental mode is shown in Figure 4.6. At $\lambda = 1.55\mu m$, this fiber provides a very large negative dispersion of -395 $ps / nm.km$. Since $\lambda = 1.55\mu m$ is close to the fundamental mode's own cutoff wavelength, the dispersion varies greatly with wavelength. Varying the wavelength from $1.54\mu m$ to $1.56\mu m$, the dispersion changes from -337 $ps / nm.km$ to -482 $ps / nm.km$, respectively. This fiber is useful for upgrading the older generation optical fiber communication systems designed to operate at $\lambda = 1.3\mu m$. The reason for such large negative dispersion is attributed to the fact that the LP_{01} mode has a cutoff wavelength of about $1.6\mu m$ which is close to the wavelength of operation $1.55\mu m$. The existence of this cutoff could have been predicted from (3.61). At $\lambda = 1.55\mu m$,

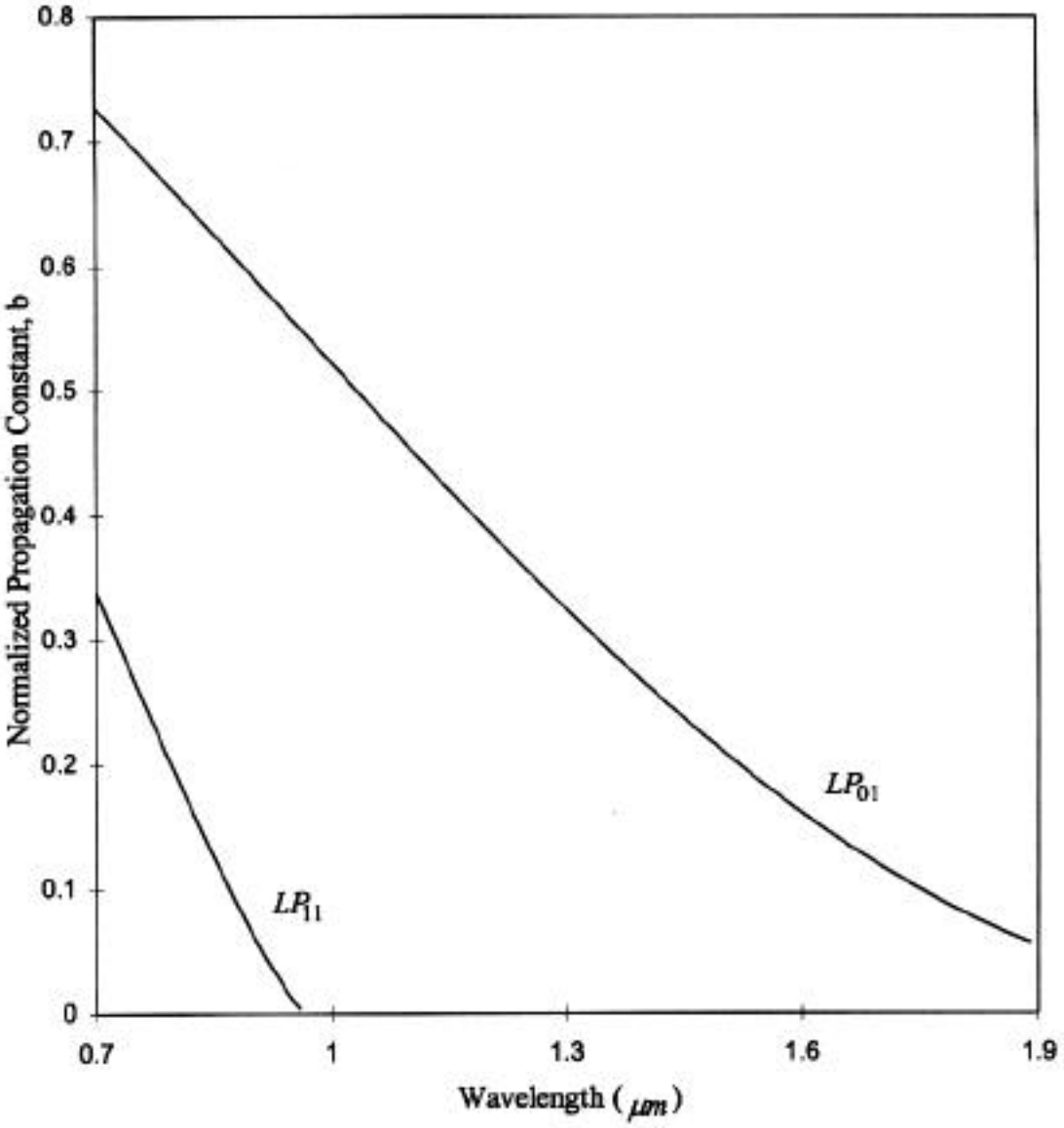

Figure 4.1 Normalized propagation constant versus wavelength for the LP_{01} and LP_{11} modes of fiber 1. Specifications of fiber 1 are given in Table 4.2.

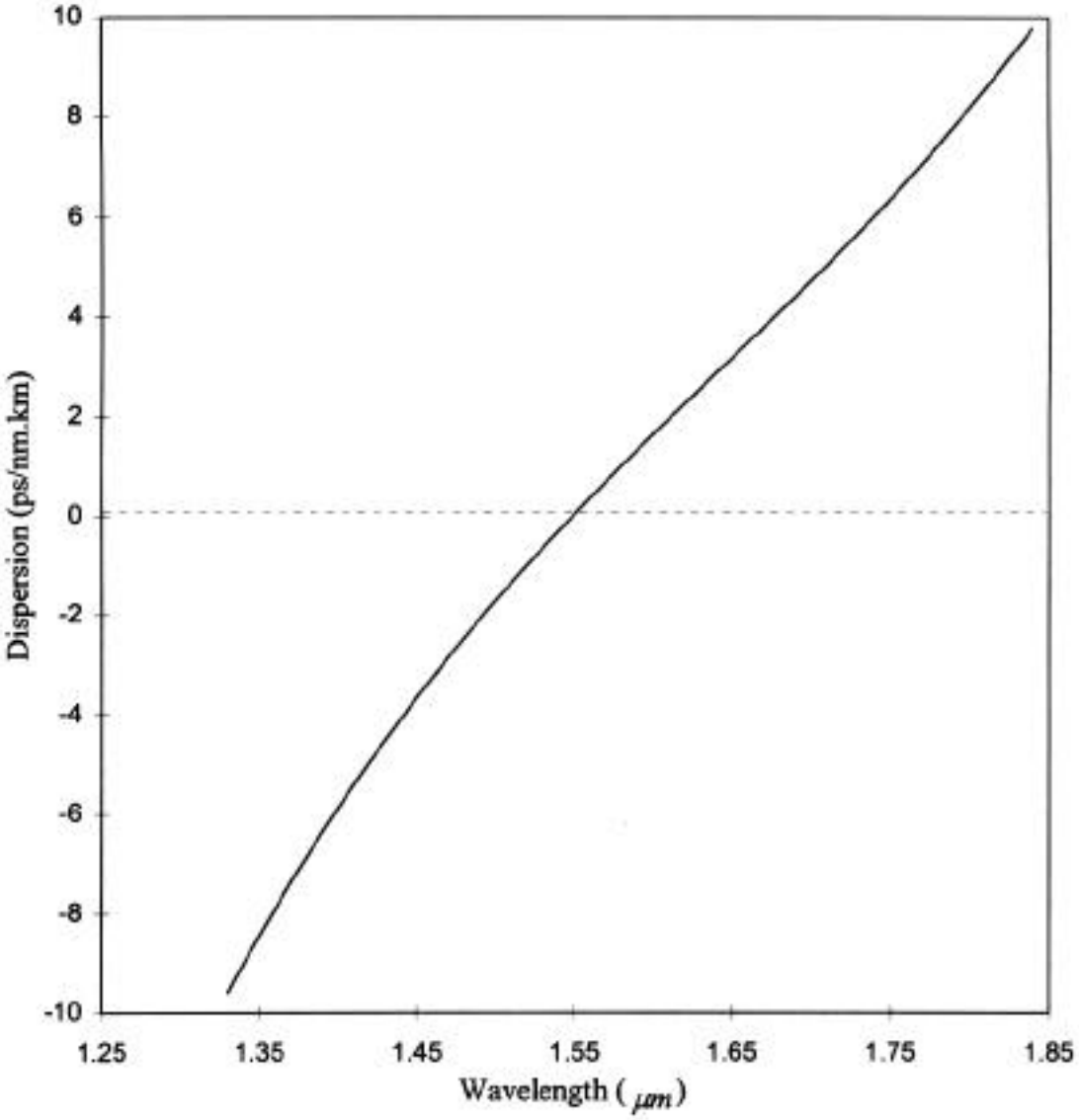

Figure 4.2 Dispersion versus wavelength for the LP_{01} mode of fiber 1. Specifications of fiber 1 are given in Table 4.2.

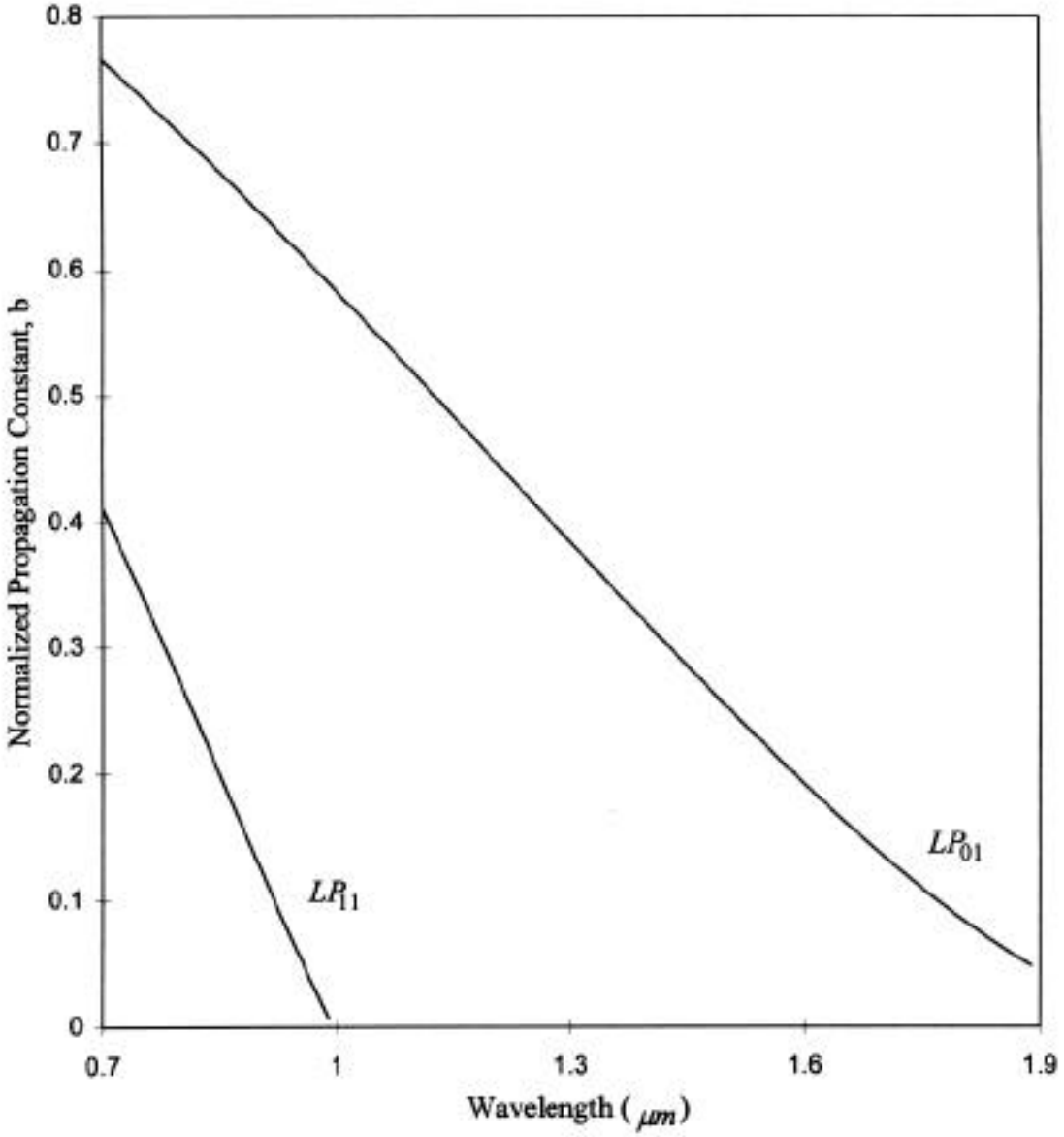

Figure 4.3 Normalized propagation constant versus wavelength for the LP_{01} and LP_{11} modes of fiber 2. Specifications of fiber 2 are given in Table 4.2.

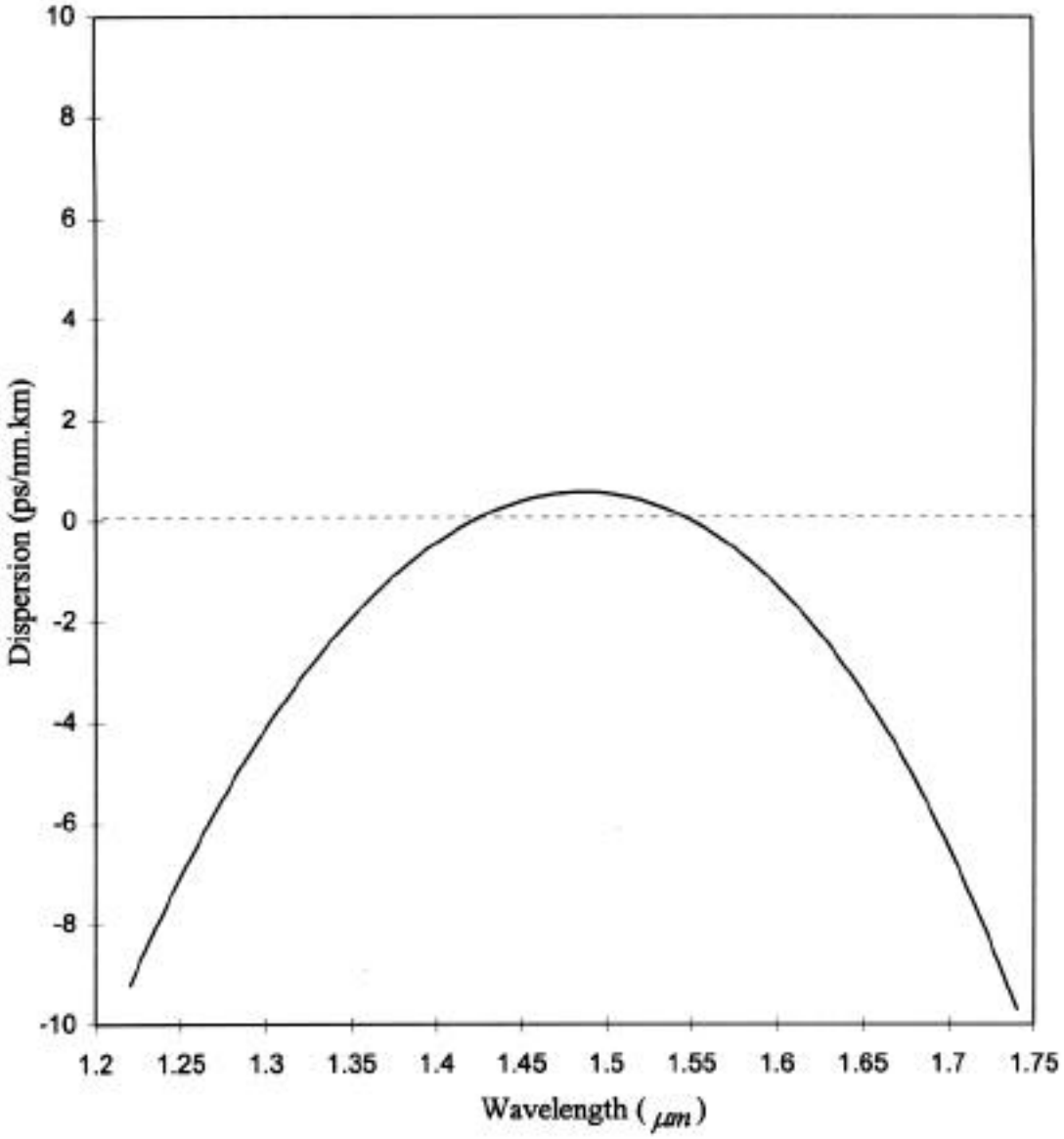

Figure 4.4 Dispersion versus wavelength for the LP_{01} mode of fiber 2. Specifications of fiber 2 are given in Table 4.2.

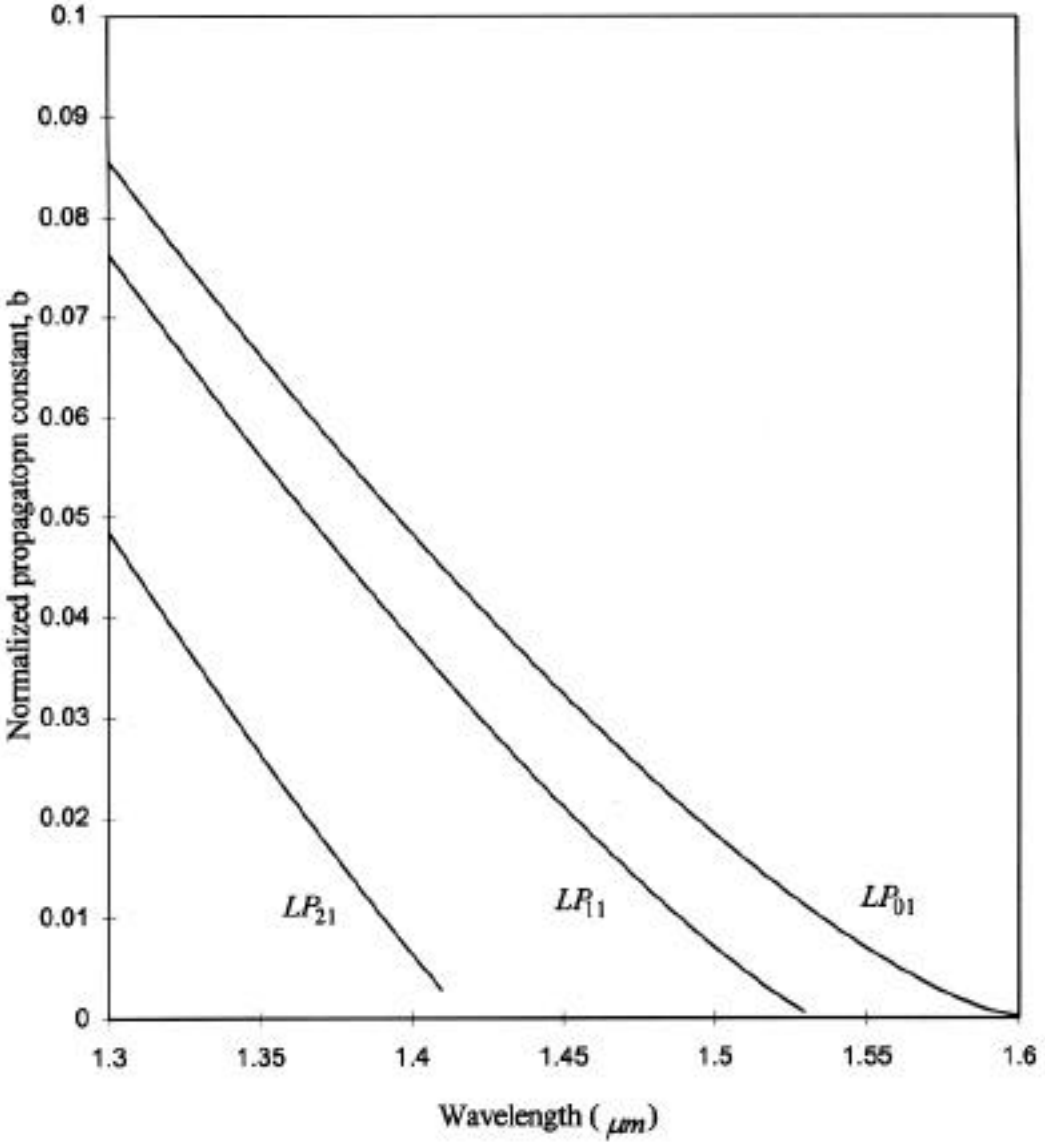

Figure 4.5 Normalized propagation constant versus wavelength for the LP_{01}, LP_{11}, and LP_{21} modes of fiber 3. Specifications of fiber 3 are given in Table 4.2.

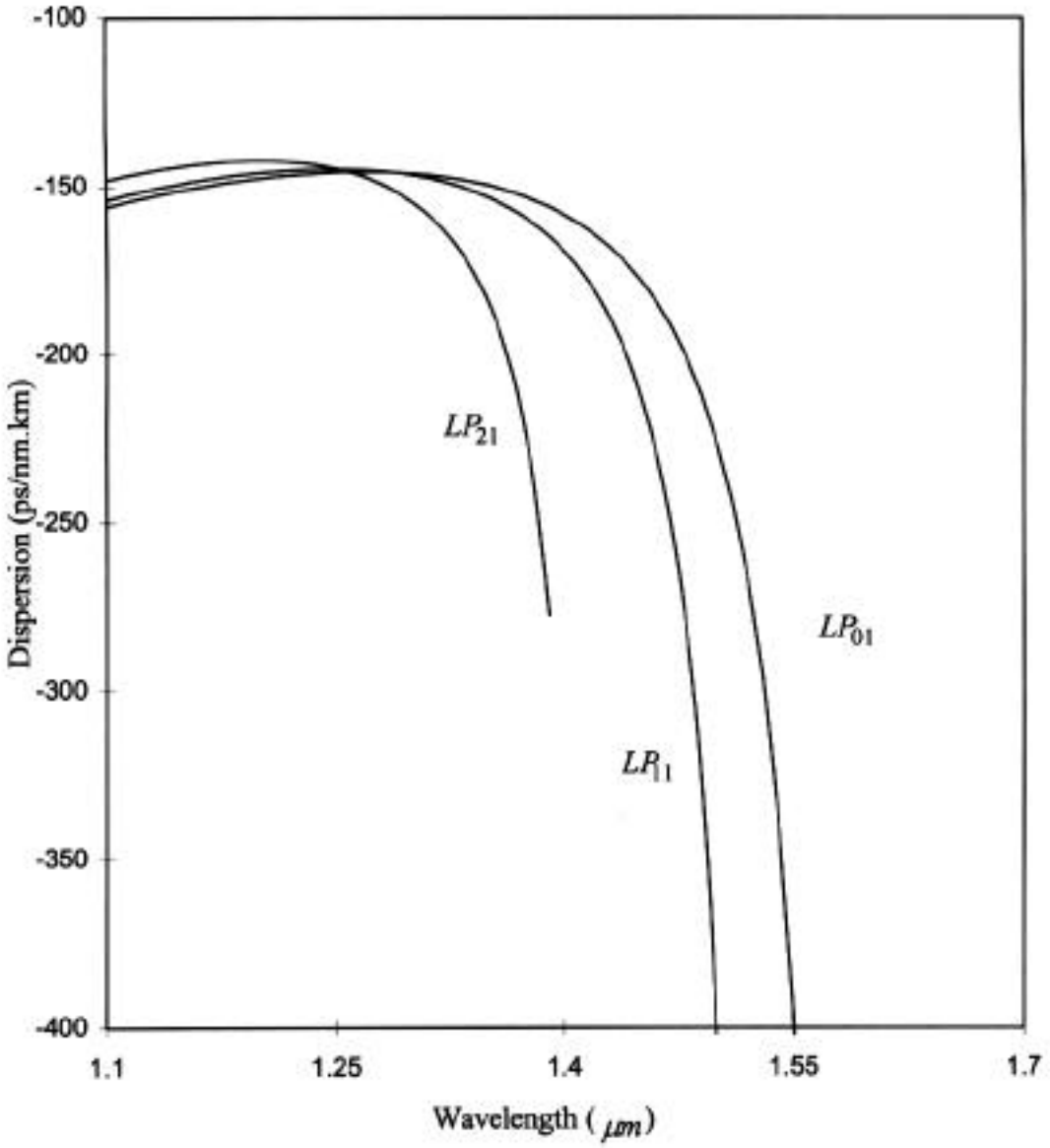

Figure 4.6 Dispersion versus wavelength for the LP_{01} mode of fiber 3. Specifications of fiber 3 are given in Table 4.2.

the indices of fiber 3 are $n_1 = n_3 = 1.439424$, $n_2 = 1.507710$, and $n_4 = 1.458942$. Accordingly, the index differences defined in (3.57) to (3.60) are obtained as $\Delta_1 = \Delta_3 = 0.0443$, $\Delta_3' = 0.0125$, and $\Delta_4 = 0.0318$. Then, with $r_1 = 5.3\mu m$, $r_2 = 6.0\mu m$, and $r_3 = 7.4\mu m$, it can be verified that the right-hand side of (3.61) is equal to 0.0443, while the left-hand side of it is equal to 0.05358. That is, (3.61) is satisfied for fiber 3.

D. Optimum Dispersion-Shifted Design

Conventional dispersion-shifted fibers such as fiber 1 provide zero second-order dispersion. The non-zero third-order dispersion causes signal distortion, particularly over long distances. To address the significance of third-order dispersion, we examine the Taylor series expansion of $\beta(\lambda)$ about $\lambda = \lambda_0$,

$$\beta(\lambda) = \beta(\lambda_0) + (\lambda - \lambda_0)\left.\frac{d\beta}{d\lambda}\right|_{\lambda=\lambda_0} + \frac{(\lambda-\lambda_0)^2}{2!}\left.\frac{d^2\beta}{d\lambda^2}\right|_{\lambda=\lambda_0} + \frac{(\lambda-\lambda_0)^3}{3!}\left.\frac{d^3\beta}{d\lambda^3}\right|_{\lambda=\lambda_0} + \ldots \quad (4.3)$$

where λ_0 is the wavelength of interest, say $1.55\mu m$. The second term involving $d\beta / d\lambda$ in the expansion represents group delay, while the third term accounts for the group delay difference and hence spreading or dispersion of the pulse envelope of the optical signal. The quantity known as second-order dispersion is defined in terms of $d^2\beta / d\lambda^2$. In most applications, the third and higher-order derivatives in (4.3) are neglected. However, if $d^2\beta / d\lambda^2$ at the wavelength of operation $\lambda = \lambda_0$ vanishes, the third-order dispersion involving $d^3\beta / d\lambda^3$ must be used in assessing pulse spreading [19]. In conventional dispersion-shifted fibers $d^2\beta / d\lambda^2$ vanishes at $\lambda_0 = 1.55\mu m$, hence significant reduction in pulse spreading. The optimum dispersion-shifted design proposed here involves developing a fiber whose second and third-order dispersions vanish simultaneously at $\lambda_0 = 1.55\mu m$. Fiber 4, with parameters shown in Table 4.2, is such a fiber. With the LP_{11} mode having a

cutoff at $\lambda = 0.87\mu m$, and all other modes, except for the fundamental LP_{01} mode, in cutoff over the range of wavelength $0.87\mu m < \lambda < 1.85\mu m$, as seen in Figure 4.7, fiber 4 is strictly single-mode over the above range of wavelengths. Dispersion characteristics versus wavelength for the LP_{01} mode of fiber 4 is shown in Figure 4.8. At $\lambda_0 = 1.55\mu m$, both the second and third-order dispersions (i.e., slope) are very close to zero. The total dispersion remains less than $1 ps/nm.km$ over the wavelength range $1.48\mu m < \lambda < 1.61\mu m$.

4.1.2 Field Distributions

Equation (3.7) gives field expressions in various layers of the cylindrical waveguide under study. The radial field distributions are calculated at a specific wavelength. The field maximum is then normalized to unity and plotted versus radial coordinate r. Plots of radial field distributions at $\lambda = 1.55\mu m$ for the four fibers defined in Table 4.2 are shown in Figures 4.8 to 4.12.

As expected, the fields are well confined to the regions of the highest refractive index in the respective fibers. The highest index region corresponds to the core region of fibers 1 and 2 ($r < r_1$), and the first cladding layer of fibers 3 and 4 ($r_1 < r < r_2$). Radial fields reach their maxima in these layers. The information on field distribution is needed in determining the thickness of the outer cladding layer of the fiber. This cladding was assumed to extend to infinity in the model used to analyze the fiber. Practical fibers, however, must have finite outer cladding. To estimate the required thickness of this cladding, the maximum allowed field at the cladding-jacket boundary need be specified. As an example, the criterion may be that the allowed field strength at the cladding-jacket boundary shall not exceed 10^{-4}% of the field maximum. Based on this criterion, the required radius of the outer cladding (i.e. fiber radius) for fibers 1, 2, 3, and 4 is calculated as $352\mu m$,

$263\mu m$, $628\mu m$, and $27\mu m$, respectively. We note that all these radii are less than (or almost equal to, for fiber 3) $625\mu m$, which is a typical radius for single mode fibers.

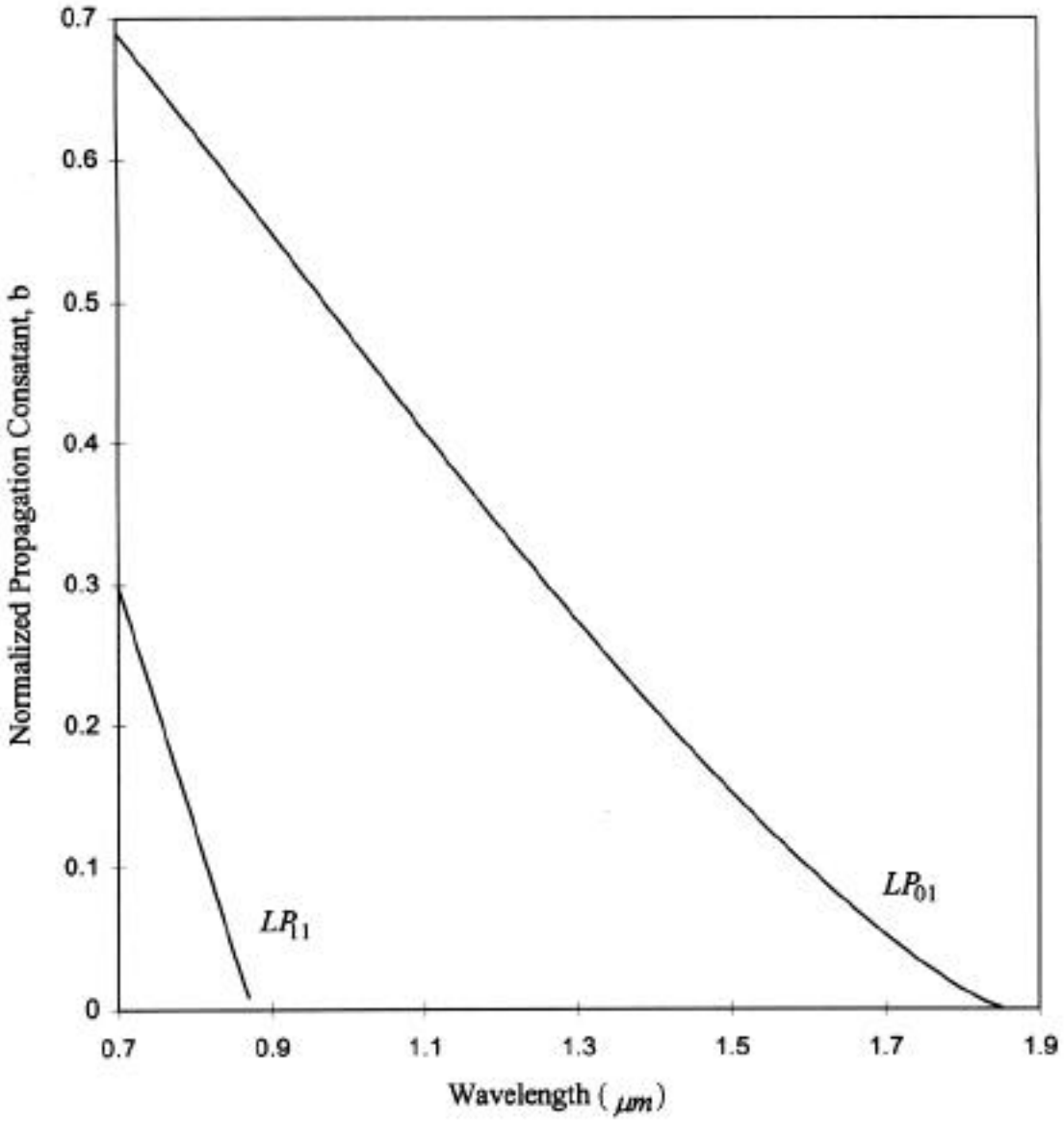

Figure 4.7 Normalized propagation constant versus wavelength for the LP_{01} and LP_{11} modes of fiber 4. Specifications of fiber 4 are given in Table 4.2.

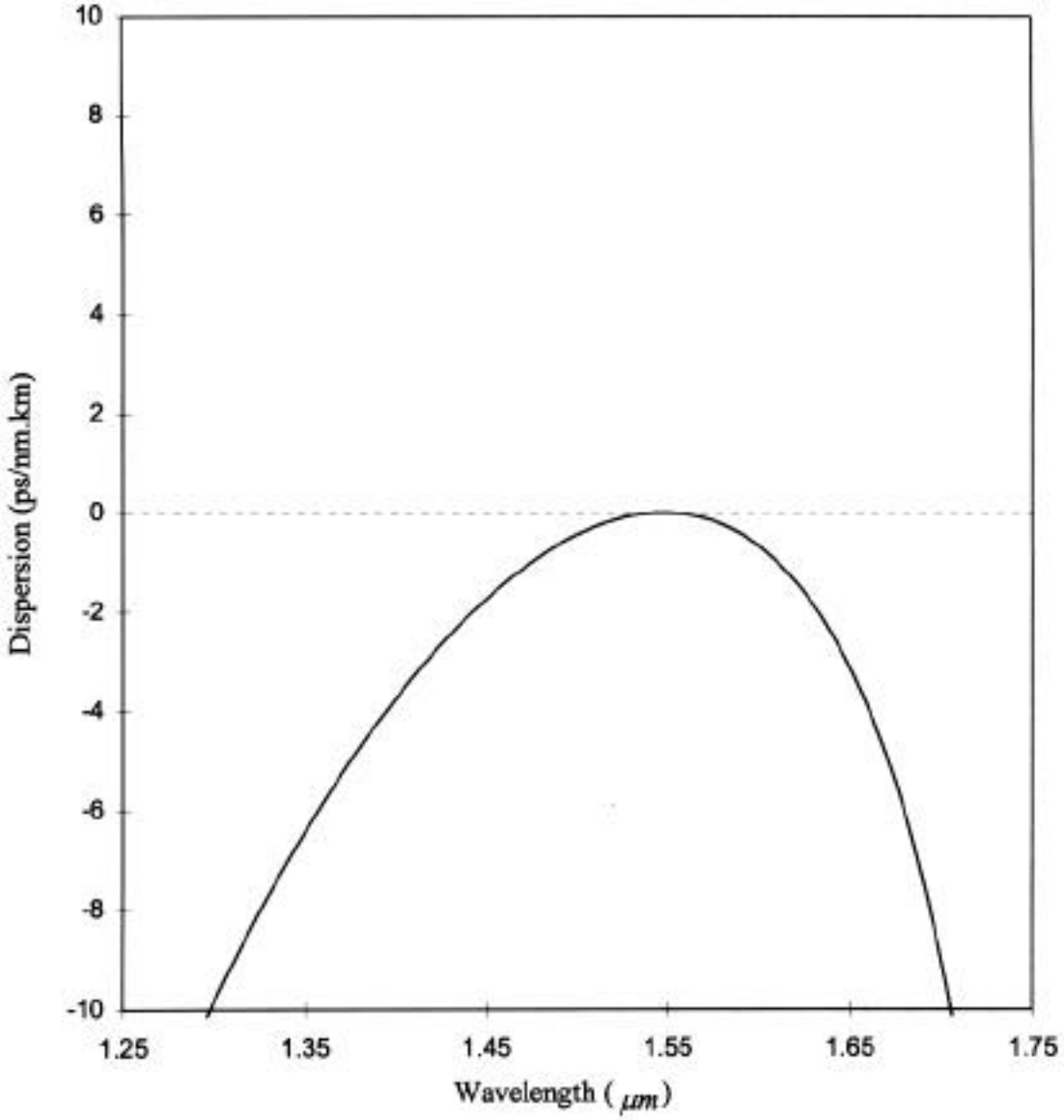

Figure 4.8 Dispersion versus wavelength for the LP_{01} mode of fiber 4. Specifications of fiber 4 are given in Table 4.2.

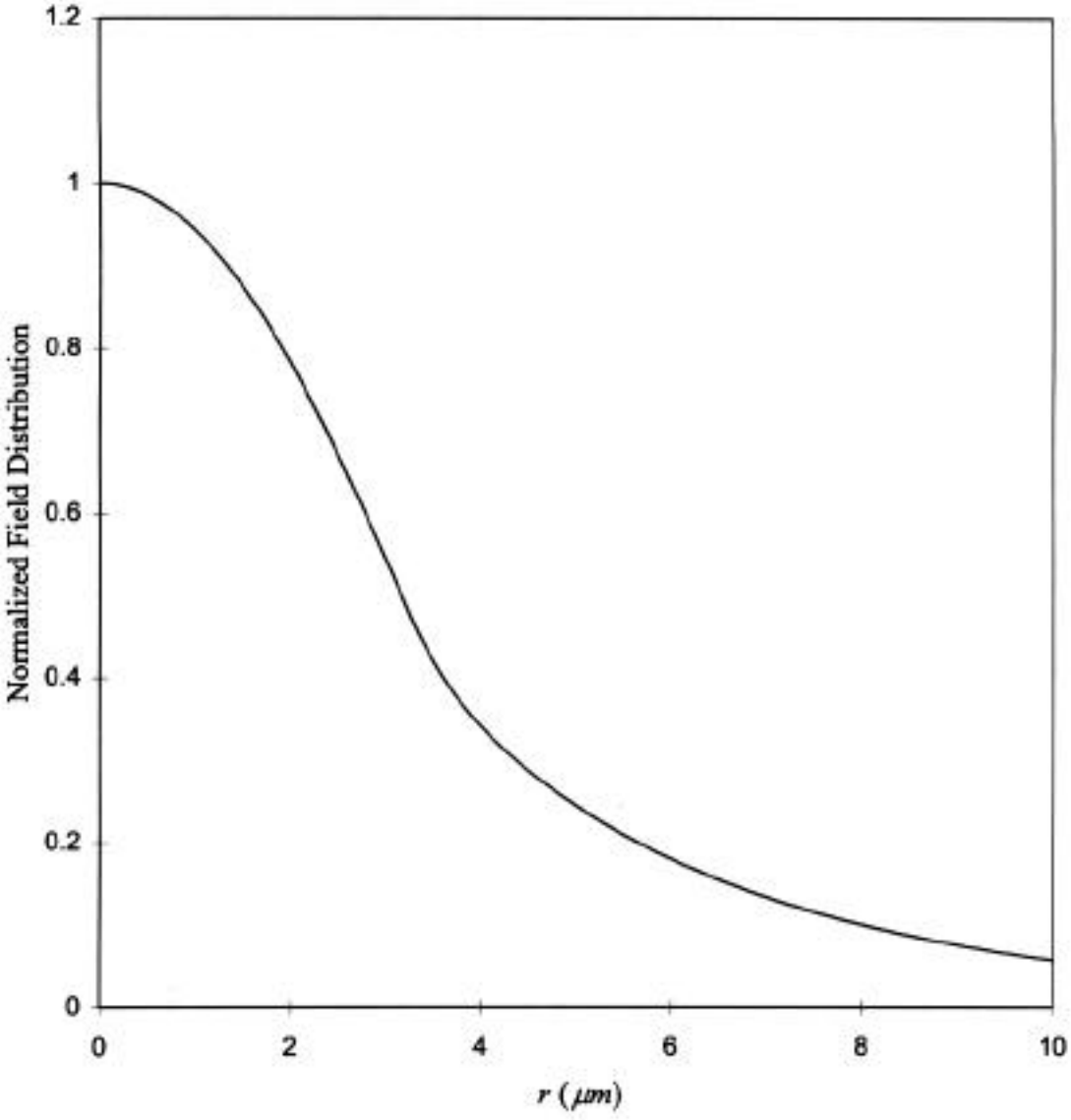

Figure 4.9 Normalized radial field distribution for the LP_{01} mode of fiber 1 at $\lambda = 1.55\mu m$. Specifications of fiber 1 are given in Table 4.2.

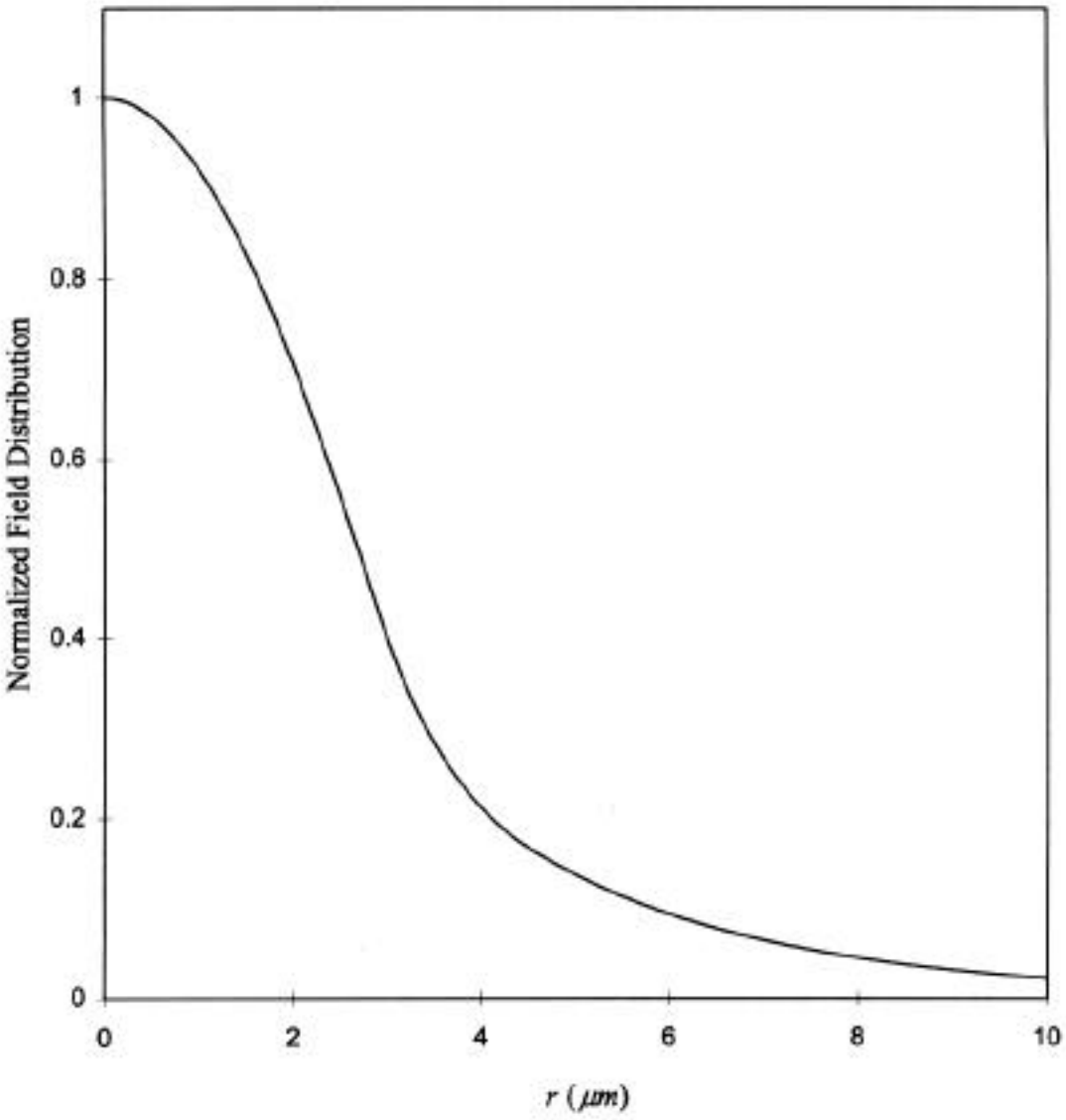

Figure 4.10 Normalized radial field distribution for the LP_{01} mode of fiber 2 at $\lambda = 1.55\mu m$. Specifications of fiber 2 are given in Table 4.2.

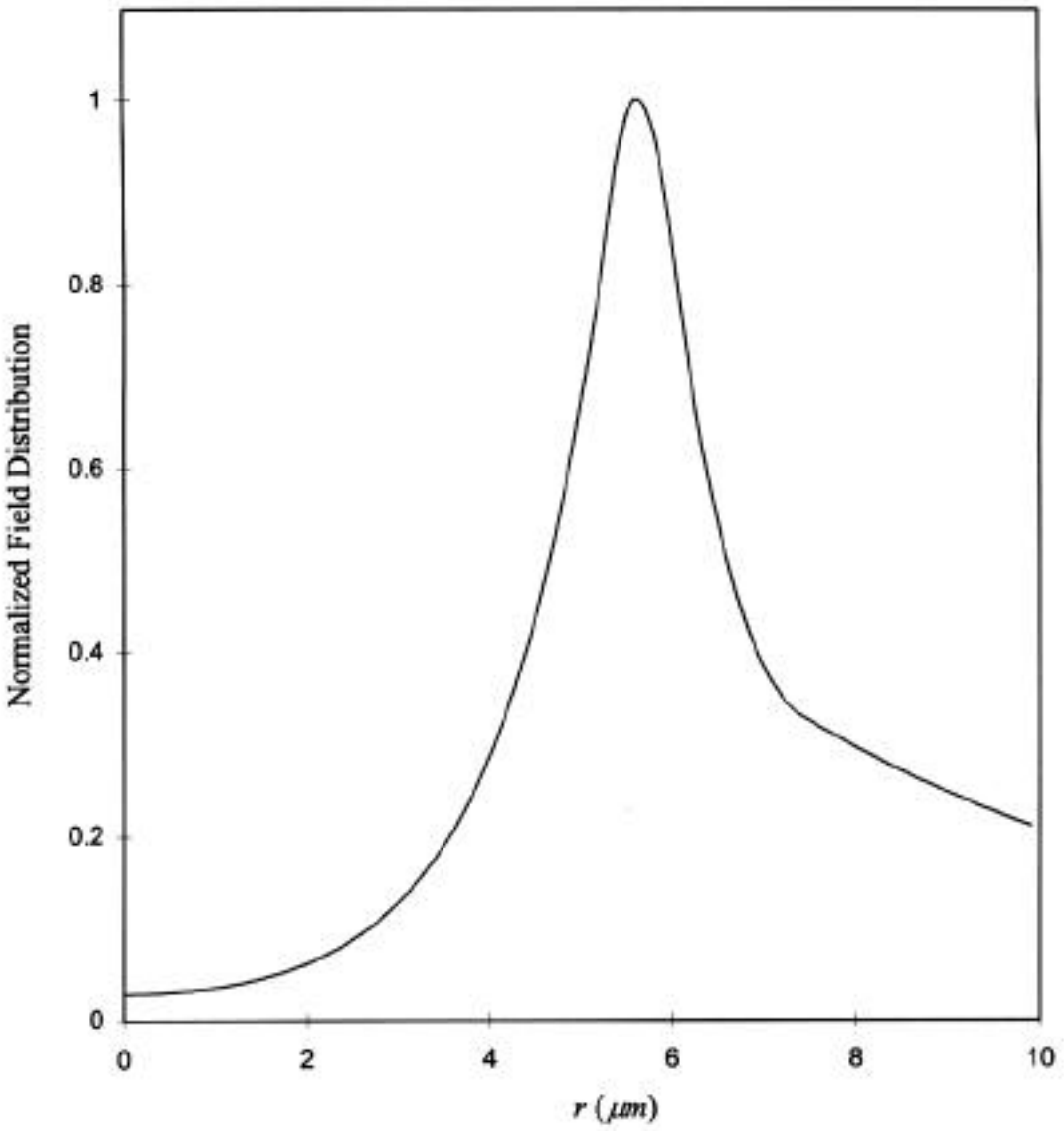

Figure 4.11 Normalized radial field distribution for the LP_{01} mode of fiber 3 at $\lambda = 1.55\mu m$. Specifications of fiber 3 are given in Table 4.2.

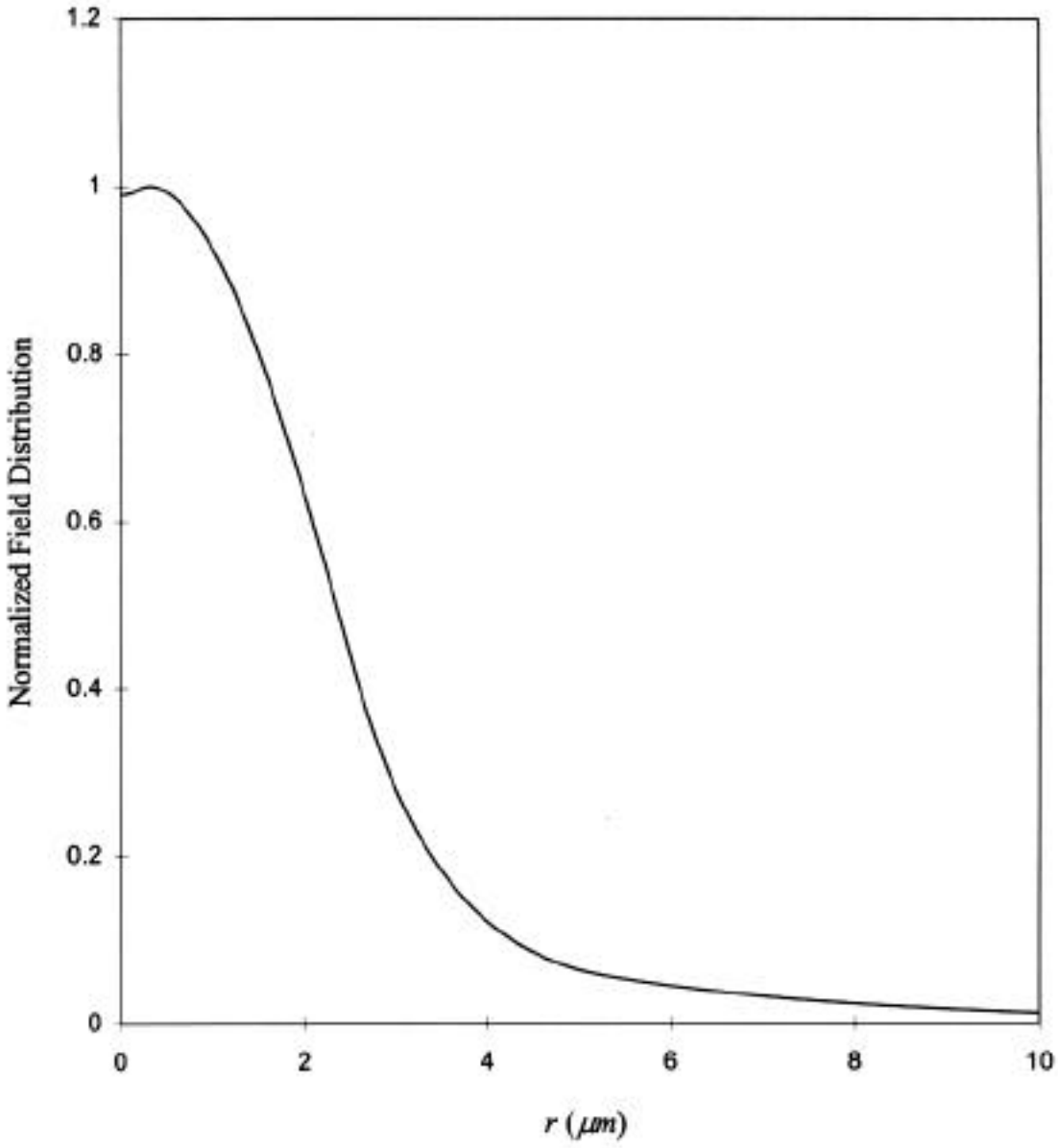

Figure 4.12 Normalized radial field distribution for the LP_{01} mode of fiber 4 at $\lambda = 1.55\mu m$. Specifications of fiber 4 are given in Table 4.2.

Chapter 5. Conclusions and Suggestions for Further Work

5.1 Conclusions

A generalized analysis of multiple-clad step-index optical fibers, with emphasis on triple-clad structures, was presented. Unified general formulations were developed to study various transmission properties of single-mode weakly guiding cylindrical optical waveguides with one, two, or three claddings, with step-index but otherwise arbitrary profiles. Specific designs to achieve dispersion-shifting, dispersion-flattening, and dispersion compensation were proposed and analyzed. In particular, optimum designs for dispersion-shifted and dispersion compensating fibers were addressed.

The optimized dispersion compensating fiber, exhibits a large negative dispersion of about -400 $ps/nm.km$ at $\lambda = 155\mu m$. This fiber has a depressed core index and the first inner cladding assumes the largest index. The advantage of this design is that it offers dispersion compensating for the fundamental LP_{01} mode, and hence the complications associated with mode coupling encountered in conventional dual-mode dispersion compensating fibers are avoided.

Also, a dispersion-shifted fiber was optimized to provide zero second-order and third-order dispersions at $\lambda = 155\mu m$. Hence, a much smaller pulse spreading occurs

compared to conventional dispersion-shifted fibers for transmission over long distances. This fiber could also be used as a dispersion-flattened fiber as it offers a low total dispersion of less than $1\ ps/nm.km$ over wavelength range of $1.48\mu m \le \lambda \le 1.61\mu m$.

5.2 Suggestions for Further Research

The generalized analysis and formulations presented in this thesis were limited to triple-clad geometries. The formulation may be extended to multiple-clad fibers with N layers and arbitrary index profiles. This formulation would be capable of handling graded-index fibers too. The scope of optimization may be widened to include other effects such as bending, microbending, and splice losses as well as nonlinear effects. The optimization accounting for nonlinear effects is particularly worth a thorough examination.

REFERENCES

[1] L. G. Cohen, C. Lin, W. G. French, "Tailoring zero chromatic dispersion into the $1.5-1.6\mu m$ low-loss spectral region of single-mode fibers," Electron. Lett., vol. 15, pp. 334-335, 1979.

[2] K. I. White, and B. P. Nelson, "Zero total dispersion in step-index monomode fibers at 1.30 and 1.55 μm," Electron. Lett., vol. 15, pp. 396-397, 1979.

[3] V. A. Bhagavatula, J. E. Ritter, and R. A. Modavis, "Bend-optimized dispersion-shifted single-mode designs," J. Lightwave Technology, vol. 13, pp. 954-957, 1985.

[4] K. Okamoto, T. Edahiro, K. Kawana, and T. Miya, "Dispersion minimization in single-mode fibers over a wide spectral range," Electron. Lett., vol. 15, pp. 729-731, 1979.

[5] L. G. Cohen, W. Mammel, S. J. Jang, "Low-loss quadruple-clad single-mode lightguides with dispersion below $2 ps/nm.km$ over the $1.28\mu m-1.65\mu m$ wavelength range," Electron. Lett., vol. 18, pp. 1023-1024, 1982.

[6] B. J. Ainslie and C. R. Day, "A review of single-mode fibers with modified dispersion characteristics," J. Lightwave Technology, vol. 4, pp. 967-979, 1986.

[7] A. Safaai-Jazi and L. J. Lu, "Evaluation of chromatic dispersion in W-type fibers," Optics Letters, vol. 14, pp. 760-762, 1989.

[8] A. Safaai-Jazi and L. J. Lu, "Approximate methods for evaluation of chromatic dispersion in dispersion-flattened fibers," J. Lightwave Technology, vol. 8, pp. 1145-1150, 1990.

[9] C. D. Poole, J. M. Wiesenfeld, D. J. DiGiovanni, and A. M. Vengsarkar, “Optical fiber-based dispersion compensation using higher order modes near cutoff,” J. Lightwave Technology, vol. 12, pp. 1746-1758, 1994.

[10] A. J. Antas and D. K. Smith, “Design and characterization of dispersion compensating fiber based on LP_{01} mode,” J. Lightwave Technology, vol. 12, pp. 1739-1745, 1994.

[11] B. Wedding, B. Franz, and B. Junginger, “10 Gb/s optical transmission up to 253 km via standard single-mode fiber using the method of dispersion supported transmission,” J. Lightwave Technology, vol. 12, pp. 1720-1727, 1994.

[12] M. J. Adams, “An Introduction to Optical Waveguides,” John Wiley & Sons, Inc., New York, 1981.

[13] D. Davison, “Single-mode wave propagation in cylindrical optical fibers,” in Optical Fiber Transmission, Edited by E. E. Basch, Indianapolis, Howard W. Sams & Co., Chapter 3, 1987.

[14] M. Saifi , S. J. Jang, L. G. Cohen, and J. Stone, “Triangular profile single-mode fiber,” Optics Letters, vol. 7, pp. 43-45, 1982.

[15] S. Kawakami and N. Nishida, “Characteristics of a doubly-clad optical fibers with a low index inner cladding,” IEEE J. Quantum Electron., vol. QE-10, pp. 879-887, 1974.

[16] A. Safaai-Jazi, R. O. Claus, and L. J. Lu, “New designs for dispersion-shifted and dispersion-flattened fibers,” SPIE, vol. 1176, pp. 196-201, 1989.

[17] A. W. Snyder and J. D. Love, “Optical Waveguide Theory,” London, Chapman and Hall, 1983.

[18] D. Gloge, “Dispersion in weakly guiding fibers,” Applied Optics, vol. 10, pp. 2242-2245, 1971.

[19] M. Miyagi and S. Nishida, “ Pulse spreading in a single-mode fiber due to third-order dispersion,” Applied Optics, vol. 18, pp. 678-682, 1979.

[20] M. Abramowitz and I. A. Stegun, “Handbook of mathematical functions, with formulas, graphs, and mathematical tables,” Dover publications, inc., New York, 1970.

[21] T. Moriyama, O. Fuduka, K. Sanada, K. Inada, T. Edahiro, and K. Chida,

"Ultimately low OH content VAD optical fibers," Electron. Lett., vol. 16, pp. 699-700, Aug. 1980.

[22] H. Osanai, T. Shioda, T. Moriyama, S. Araki, M. Horiguchi, T. Izawa, and H. Takata, "Effects of dopants on transmission loss of low OH content optical fibers," Electron. Lett., vol. 12, pp. 549-550, Oct. 1976.

[23] S. J. Jang, L. G. Cohen, W. Mammel, and M. Saifi, "Experimental verification of ultra-wide bandwidth spectra in double-clad single-mode fibers," Bell Syst. Tech. J., vol. 61, pp. 385-390, 1982.

Appendix

The Bessel and modified Bessel functions of the first and second kinds used in the formulations described in Chapters 2 and 3, were calculated using polynomial approximations. These approximations for zeroth and first order Bessel and modified Bessel functions are summarized below [20].

A.1 Polynomial Approximations

For $-3 \le x \le 3$,

$$J_0(x) = 1 - 2.2499997(x/3)^2 + 1.2656208(x/3)^4 - .3163866(x/3)^6 + .0444479(x/3)^8 - .0039444(x/3)^{10} + .0002100(x/3)^{12}, \qquad \text{(A.1.1)}$$

$$x^{-1}J_1(x) = \tfrac{1}{2} - .56249985(x/3)^2 + .21093573(x/3)^4 - .03954289(x/3)^6 + .00443319(x/3)^8 - .00031761(x/3)^{10} + .00001109(x/3)^{12}. \qquad \text{(A.1.2)}$$

For $0 < x \le 3$,

$$Y_0(x) = (2/\pi)\ln(x/2)J_0(x) + .36746691 + .60559366(x/3)^2 - .74350384(x/3)^4 + .25300117(x/3)^6 - .04261214(x/3)^8 + .00427916(x/3)^{10} - .00024846(x/3)^{12}, \qquad \text{(A.1.3)}$$

$$xY_1(x) = (2/\pi)x\ln(x/2)J_1(x) - .6366198 + .2212091(x/3)^2 + 2.1682709(x/3)^4 - 1.3164827(x/3)^6 + .3123951(x/3)^8 - .0400976(x/3)^{10} + .0027873(x/3)^{12}. \qquad \text{(A.1.4)}$$

For $3 \le x < \infty$,

$$J_0(x) = x^{-\frac{1}{2}} f_0 \cos\theta_0,\ Y_0(x) = x^{-\frac{1}{2}} f_0 \sin\theta_0, \tag{A.1.5}$$

$$J_1(x) = x^{-\frac{1}{2}} f_1 \cos\theta_1,\ Y_1(x) = x^{-\frac{1}{2}} f_1 \sin\theta_1, \tag{A.1.6}$$

where

$$f_0 = .79788456 - .00000077(3/x) - .0055274(3/x)^2 - .00009512(3/x)^3 + .00137237(3/x)^4 + .00072805(3/x)^5 + .00014476(3/x)^6, \tag{A.1.7}$$

$$f_1 = .79788456 + .00000156(3/x) + .01659667(3/x)^2 + .00017105(3/x)^3 - .00249511(3/x)^4 + .00113653(3/x)^5 - .00020033(3/x)^6, \tag{A.1.8}$$

and

$$\theta_0 = x - .78539816 - .04166397(3/x) - .00003954(3/x)^2 + .00262573(3/x)^3 - .00054125(3/x)^4 - .00029333(3/x)^5 + .00013558(3/x)^6, \tag{A.1.9}$$

$$\theta_1 = x - 2.35619449 + .12499612(3/x) + .00005650(3/x)^2 - .00637879(3/x)^3 + .00074348(3/x)^4 + .00079824(3/x)^5 - .00029166(3/x)^6. \tag{A.1.10}$$

For $-3.75 \le x \le 3.75$,

$$I_0(x) = 1 + 3.5156229t^2 + 3.0899424t^4 + 1.2067492t^5 + .2659732t^8 + .0360768t^{10} + .0045813t^{12}, \tag{A.1.11}$$

$$x^{-1} I_1(x) = \tfrac{1}{2} + .87890594t^2 .51498869t^4 + .15084934t^6 + .02658733t^8 + .00301532t^{10} + .00032411t^{12}. \tag{A.1.12}$$

For $3.75 \le x < \infty$,

$$x^{\frac{1}{2}} e^{-x} I_0(x) = .39894228 + .01328592t^{-1} + .00225319t^{-2} - .00157565t^{-3}$$

$$+.00916281t^{-4} - .02057706t^{-5} + .02635537t^{-6} - .01647633t^{-7} + .00392377t^{-8},$$

(A.1.13)

$$x^{\frac{1}{2}}e^{-x}I_1(x) = .39894228 - .03988024t^{-1} - .00362018t^{-2} + .00163801t^{-3}$$
$$- .01031555t^{-4} + .02282967t^{-5} - .02895312t^{-6}.0187654t^{-7} - .00420059t^{-8},$$

(A.1.14)

where $t = x/3.75$.

For $0 < x \le 2$,

$$K_0(x) = -\ln(x/2)I_0(x) - .57721566 + .42278420(x/2)^2 + .23069756(x/2)^4$$
$$+ .03488590(x/2)^6 + .00262698(x/2)^8 + .00010750(x/2)^{10} + .0000074(x/2)^{12},$$

(A.1.15)

$$xK_1(x) = x\ln(x/2)I_1(x) + 1 + .15443144(x/2)^2 - .67278579(x/2)^4 - .18156897(x/2)^6$$
$$- .01919402(x/2)^8 - .00110404(x/2)^{10} - .00004686(x/2)^{12}.$$ (A.1.16)

For $2 \le x < \infty$,

$$x^{\frac{1}{2}}e^{x}K_0(x) = 1.25331414 - .07832358(2/x) + .02189568(2/x)^2 - .01062446(2/x)^3$$
$$+ .00587872(2/x)^4 - .00251540(2/x)^5 + .00053208(2/x)^6,$$ (A.1.17)

$$x^{\frac{1}{2}}e^{x}K_1(x) = 1.25331414 + .23498619(2/x) - .03655620(2/x)^2 + .01504268(2/x)^3$$
$$- .00780353(2/x)^4 + .00325614(2/x)^5 - .00068245(2/x)^6.$$ (A.1.18)

A.2 Recurrence Formulas for Calculations of Second and Higher-Order Bessel and Modified Bessel Functions.

$$xJ_n'(x) = xJ_{n-1}(x) - nJ_n(x)$$ (A.2.1)

$$J_n'(x) = \tfrac{1}{2}\{J_{n-1}(x) - J_{n+1}(x)\}$$ (A.2.2)

$$xI_n^{'}(x) = xI_{n-1}(x) - nI_n(x) \quad \text{(A.2.3)}$$

$$I_n^{'}(x) = \tfrac{1}{2}\{I_{n-1}(x) + I_{n+1}(x)\} \quad \text{(A.2.4)}$$

$$xK_n^{'}(x) = -xK_{n-1}(x) - nK_n(x) \quad \text{(A.2.5)}$$

$$K_n^{'}(x) = -\tfrac{1}{2}\{K_{n-1}(x) + K_{n+1}(x)\} \quad \text{(A.2.6)}$$

A.3 Other Relevant Identities for Calculations of Derivatives of Zeroth Order Bessel and Modified Bessel Functions

$$Y_{-n}(x) = (-1)^n Y_n(x) \quad \text{(A.3.1)}$$

$$J_{-n}(x) = (-1)^n J_n(x) \quad \text{(A.3.2)}$$

$$I_{-n}(x) = I_n(x) \quad \text{(A.3.3)}$$

$$K_{-n}(x) = K_n(x) \quad \text{(A.3.4)}$$

A.4 Small Argument Approximations of Bessel and Modified Bessel Functions

$$J_0(x) \to 1 \quad \text{(A.4.1)}$$

$$J_1(x) \to \tfrac{1}{2}x \quad \text{(A.4.2)}$$

$$Y_0(x) \to \tfrac{2}{\pi}\ln x \quad \text{(A.4.3)}$$

$$Y_1(x) \to -\frac{2}{\pi x} \quad \text{(A.4.4)}$$

$$I_0(x) \to 1 \quad \text{(A.4.5)}$$

$$I_1(x) \to \tfrac{1}{2}x \quad \text{(A.4.6)}$$

$$K_0(x) \to -\ln x \quad \text{(A.4.7)}$$

$$K_1(x) \to \frac{1}{x} \quad \text{(A.4.8)}$$

Vita

Taha M. Barake was born in Tripoli Lebanon in February 1966. He attended the Lebanese University for two years and then was awarded a fellowship to pursue his higher education in the US where he attended the University of Bridgeport, CT. While in college, he held an electronics laboratory technician position for two years at Vectron Labs where he worked on crystal oscillators. In 1991, he received his Bachelor of Science degree in electrical engineering. He later joined the graduate program at Virginia Polytechnic Institute and State University, where he pursued his studies and research in the area of fiber optics.